University of Alberta

Carbon-Carbon Bond Formation At Adjacent Metal Centres

By

Amala Chokshi

A thesis submitted to the Faculty of Graduate Studies and Research in partial fulfillment of the
requirements for the degree of Master of Science

Department of Chemistry

Edmonton, Alberta
Spring 2004

Library and Archives Canada
Bibliothèque et Archives Canada

Published Heritage Branch
Direction du Patrimoine de l'édition

395 Wellington Street
Ottawa ON K1A 0N4
Canada

395, rue Wellington
Ottawa ON K1A 0N4
Canada

Your file Votre référence
ISBN: 0-612-96459-0
Our file Notre référence
ISBN: 0-612-96459-0

The author has granted a non-exclusive license allowing the Library and Archives Canada to reproduce, loan, distribute or sell copies of this thesis in microform, paper or electronic formats.

L'auteur a accordé une licence non exclusive permettant à la Bibliothèque et Archives Canada de reproduire, prêter, distribuer ou vendre des copies de cette thèse sous la forme de microfiche/film, de reproduction sur papier ou sur format électronique.

The author retains ownership of the copyright in this thesis. Neither the thesis nor substantial extracts from it may be printed or otherwise reproduced without the author's permission.

L'auteur conserve la propriété du droit d'auteur qui protège cette thèse. Ni la thèse ni des extraits substantiels de celle-ci ne doivent être imprimés ou aturement reproduits sans son autorisation.

In compliance with the Canadian Privacy Act some supporting forms may have been removed from this thesis.

Conformément à la loi canadienne sur la protection de la vie privée, quelques formulaires secondaires ont été enlevés de cette thèse.

While these forms may be included in the document page count, their removal does not represent any loss of content from the thesis.

Bien que ces formulaires aient inclus dans la pagination, il n'y aura aucun contenu manquant.

Canada

Abstract

The complex $[RhOs(CO)_3(\mu\text{-}CH_2)(dppm)_2][X]$ (**2.1**) is prepared by treatment of $[RhOs(CO)_4(\mu\text{-}CH_2)(dppm)_2][X]$ (**1.2** dppm = $Ph_2PCH_2PPh_2$, X = BF_4^-, $CF_3SO_3^-$) with Me_3NO. Compound **1.2** proved unreactive toward alkyne incorporation, whereas **2.1** incorporates alkynes into the metallic framework, yielding $[RhOs(CO)_3(\mu\text{-}\eta^1\text{:}\eta^1\text{-}C(R)=C(R)CH_2)(dppm)_2][X]$ (R, = CO_2Me (**2.2**), CF_3 (**2.3**)) each with a bridging C_3 fragment. Compound **2.2** reacts further with diazomethane, giving a C_4-bridged product, $[RhOs(CO)_3(\mu\text{-}\eta^1\text{:}\eta^1\text{-}CH_2(MeO_2C)C=C(CO_2Me)CH)(\mu\text{-}H)(dppm)_2][CF_3SO_3]$ (**2.7**). The addition of diazomethane to the alkyne-bridged compound $[RhOs(CO)_3(\mu\text{-}\eta^1\text{:}\eta^1\text{-}(CO_2Me)C=C(CO_2Me))(dppm)_2][X]$, gave two different isomers of **2.2**.

Compound **2.1** reacts with allenes to give the complexes $[RhOs(CO)_2(\mu\text{-}\eta^3\text{:}\eta^1\text{-}C(CH_2)_3)(dppm)_2][X]$ (**3.1**), $[RhOs(CO)_2(\mu\text{-}\eta^3\text{:}\eta^1\text{-}(CH_3)HCC(CH_2)_2)(dppm)_2][X]$ (**3.4**), and $[RhOs(CO)_3(\mu\text{-}\eta^1\text{:}\eta^1\text{-}(CH_3)_2CCH_2CH_2)(dppm)_2][CF_3SO_3]$ (**3.6**). The methyl substituent in **3.4** is found to have an agostic interaction with Rh. Addition of CO and PMe_3 to **3.1** gives the complexes $[RhOs(CO)_2(L)(\mu\text{-}\eta^3\text{:}\eta^1\text{-}C(CH_2)_3)(dppm)_2][X]$ (L = CO (**3.2**), PMe_3 (**3.3**)), while only CO coordinates to **3.4**, replacing the agostic methyl.

A rationalization for the above chemistry and the roles of the different metals is presented.

It was the best of times, it was the worst of times.

-Charles Dickens *A Tale of Two Cities*

Acknowledgements

First and foremost, I would like to thank my supervisor Marty for all his help and patience, especially during the thesis writing. I also appreciate that you learned to say my first name, although it was seldom used.

To the boys of the Cowie group (in no particular order): Steve, Wiggy, Bryan, Jay, Jim, Dusan, Rahul, and all others who have passed through during my time here, thanks for all your help, 'witty' banter, and camaraderie. Keep up the good work! I would also like to thank Camp X-ray (Bob and Mike) for the crystallography, and also for their friendship and coffee breaks.

I am also grateful to all the service staff personnel who have run experiments for me; namely the staff in the NMR, Spectral Services, Mass Spectrometry, and Elemental Analysis labs. I'd also like to thank my friends who have all helped me in their own special way.

Finally, to my family, I'd like to say thank-you for your love and support.

Table of Contents

Chapter 1

Introduction 1

References and Notes 16

Chapter 2

Introduction 19

Experimental 20

Preparation of Compounds 21

Results and Compound Characterization 28

Discussion 46

Conclusions 54

References and Notes 55

Chapter 3

Introduction 58

Experimental 59

Preparation of Compounds 59

Results and Compound Characterization 65

Discussion 75

Conclusions 82

References and Notes 83

Chapter 4

Conclusions and Future Work 85

References and Notes 91

Appendix 92

List of Tables

Chapter 2

Table 2.1 Spectroscopic Data for the Compounds 22

Table 2.2 Crystallographic Experimental Details 29

Table 2.3 Selected Distances and Angles for $[RhOs(CO)_3(\mu\text{-}(CO_2CH_3)C{=}C(CO_2CH_3)(dppm)_2]^+$ 36

Table 2.4 Selected Distances and Angles for $[RhOs(CO)_3(\mu\text{-}(CF_3)C{=}C(CF_3)(dppm)_2]^+$ 40

Chapter 3

Table 3.1 Spectroscopic Data for the Compounds 60

List of Schemes and Figures

Chapter 1

Scheme 1.1. 2

Scheme 1.2. 3

Scheme 1.3. 4

Scheme 1.4. 5

Scheme 1.5. 7

Scheme 1.6. 8

Scheme 1.7. 12

Scheme 1.8. 13

Figure 1.1. *Perpendicular and parallel alkyne binding modes in bimetallic systems.* 10

Figure 1.2. *Example of an alkyne-bridged dimetallic system.* 10

Figure 1.3. *A C_3-bridged dimetallic system.* 11

Figure 1.4. *The framework of generic dppm-bridged "A-frame" complexes.* 14

Chapter 2

Scheme 2.1. 33

Scheme 2.2. 45

Scheme 2.3. 48

Scheme 2.4. 50

Scheme 2.5. 51

Figure 2.1. *Perspective view of* $[RhOs(CO)_3(\mu,\eta^1:\eta^1\text{-}(CO_2CH_3)C{=}C\text{-}(CO_2CH_3))(dppm)_2]^+$. 35

Figure 2.2. *Perspective view of* $[RhOs(Cl)(CO)_2(\mu,\eta^1:\eta^1\text{-}(CF_3)\ C{=}C(CF_3))\text{-}(dppm)_2]^+$. 39

Figure 2.3. *Two configurations of* C_3*-bridged complexes.* 43

Chapter 3

Scheme 3.1. 66

Scheme 3.2. 66

Scheme 3.3. 69

Scheme 3.4. 73

Scheme 3.5. 76

Scheme 3.6. 79

Scheme 3.7. 81

List of Abbreviations and Symbols

anal	analysis
approx.	approximately
ca.	circa (approximately)
calcd	calculated
cont'd	continued
COSY	Correlation Spectroscopy
δ	Chemical Shift
DMA	1,1-dimethylallene
DMAD	dimethyl acetylenedicarboxylate
dppm	bis(diphenylphosphino)methane
equiv	equivalent
Et	ethyl
FT	Fischer-Tropsch
HMBC	Heteronuclear Multiple Bond Correlation
HMQC	Heteronuclear Multiple-Quantum Coherence Experiment
IR	infrared
Me	methyl
mg	milligram
min	minute
mL	millilitres
mmol	millimoles

MHz	megahertz
NMR	nuclear magnetic resonance
Ph	phenyl
THF	tetrahydrofuran
TMNO	trimethylamine N-Oxide
μL	microlitres

Chapter 1.

Introduction

The formation of carbon-carbon bonds is of fundamental importance in chemistry, being critical in the synthesis of complex organic molecules from smaller, simpler ones. Industrially, there are many processes based on carbon-carbon bond formation, including olefin hydroformylation,[1a] methanol carbonylation,[1a] olefin polymerization,[1b] and the Fischer-Tropsch (**FT**) reaction.[1] As expressed in Equation 1, **FT** reaction transforms synthesis gas ($CO + H_2$) into linear alkanes, α-olefins, and oxygen-containing products such as ethanol and aldehydes, over a heterogeneous catalyst.

$$CO + H_2 \xrightarrow{\text{catalyst}} C_nH_{2n+2} + C_nH_{2n} + \text{oxygenates} + H_2O \qquad (1)$$

The historical importance of the Fischer-Tropsch process was established during the Second World War, during which Germany used their abundant coal supplies to generate synthesis gas, which was subsequently transformed into diesel fuel using **FT** technology.[1a] Subsequent to this, the **FT** process was used in South Africa to generate fuels from their coal reserves during the oil embargo, which prevented their access to conventional oil reserves.[1a] Currently, even with relatively abundant supplies of conventional oil, the **FT** process is finding use in the conversion of "stranded" natural gas supplies into synthesis gas and subsequently into chemical feedstocks.[2] The so-called "gas-to-liquid" transformation is rapidly gaining importance, as conventional reserves become depleted.[2]

Although the **FT** process has been known for almost a century, the mechanisms of product formation are still not well understood, despite the numerous proposals that have been put forth to rationalize the different products obtained.[3] In the case of alkane and alkene formation, the **FT** process can be broken down into two steps. The first step involves cleavage of the C-O bond of carbon monoxide and subsequent transformation of the resulting carbide moiety into C_1-containing hydrocarbyl species such as methyne, methylene, and methyl groups bound to the catalyst surface, as shown in Scheme 1.1.

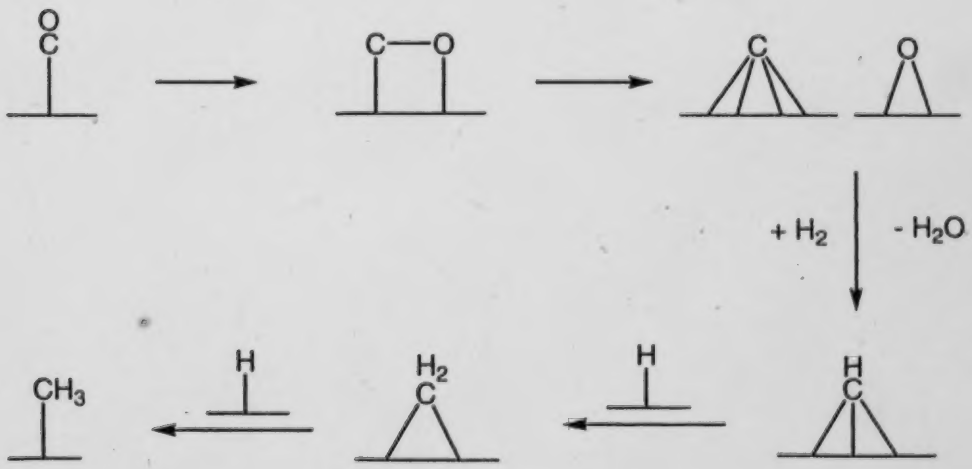

Scheme 1.1. *A simplified diagram for the conversion of syn gas into hydrocarbyl groups. The metal surface in this and subsequent schemes is designated by a horizontal line.*

The main uncertainty in the **FT** process concerns the mechanism of formation of higher hydrocarbons through coupling of the above C_1 hydrocarbyl fragments. A number of schemes have been put forward to rationalize the formation of higher hydrocarbons. The first proposal by Fischer and Tropsch suggested that the direct coupling of methylene groups yielded polymethylene oligomers.[3c] However, Brady and Pettit showed that the simple coupling of multiple methylene units on a metal surface did not seem to occur.[3d,e]

When diazomethane, a source of methylene groups, was passed over the metal catalyst it was discovered that only ethylene formed. The formation of the appropriate **FT** distribution of products required the presence of *both* diazomethane-generated methylene groups *and* H_2.[3c] From these observations it was concluded that H_2 was required for conversion of some methylene groups into methyl groups, which could migrate to an adjacent methylene group[3d] as shown in Scheme 1.2. Subsequent migration of ethyl to methylene groups generated propyl groups and so on. They proposed that chain termination occurred either by combination of a surface-bound alkyl group and a surface hydride to yield the corresponding alkane, or by β-hydride elimination to yield the α-olefin. Both types of products are obtained in **FT** chemistry.

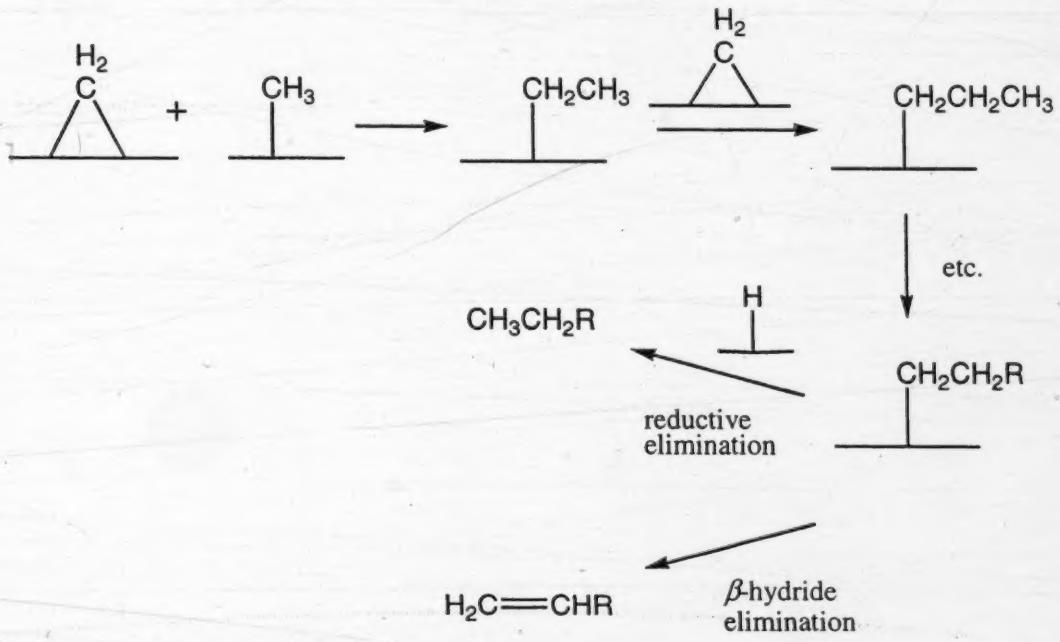

Scheme 1.2. *The Brady-Pettit mechanism for chain growth and formation of linear alkanes and α–olefins in the FT reaction.*

A more recent theory explaining the **FT** mechanism was put forth by Maitlis and co-workers who proposed that the chain propagation steps involves coupling of methylene and vinyl groups.[4] On the basis of studies on model methylene-bridged Rh_2 complexes, the surface-bound vinyl groups (or alkenyl) groups were proposed to result from either coupling of methyne and methylene groups,[5] or could result from the C-H activation of ethylene, a possible product in the **FT** reaction. In this "alkenyl" mechanism, shown in Scheme 1.3, in which the surface vinyl group is generated from methylene and methyne groups, the chain propagation steps involve coupling of a vinyl group with an adjacent methylene to form an allyl fragment. Isomerization of the allyl group by a 1,3 hydrogen shift generates a substituted vinyl group that can lead to longer-chain α-olefins by subsequent insertion and isomerization steps. The "alkenyl mechanism" of Maitlis recognized the apparent difference in mechanism of formation of

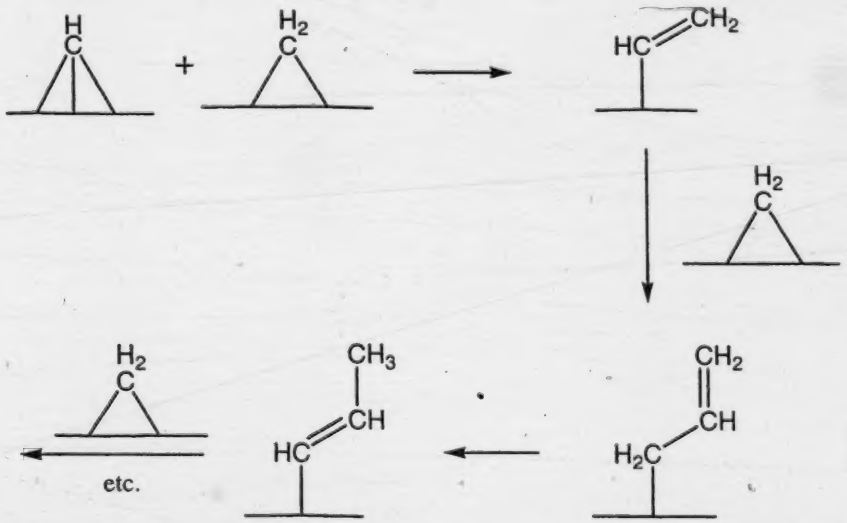

Scheme 1.3. *Maitlis' "alkenyl" mechanism for initiation and chain growth in the FT reaction*

the C_2 fragments compared to higher oligomers, as shown by the anomalously low yield of C_2 products in the **FT** reaction.[5] An alternate proposal to explain the anomalously low yields of C_2 products has recently been put forward by Dry, who suggested that the chain-propagation steps result from coupling of surface-bound olefins with surface-bound methylene groups.[6] Again the mechanism of formation of the C_2 product differs from that of subsequent steps. In the first chain-propagation step, coupling of ethylene and methylene groups occurs to give a C_3H_6 (propanediyl) fragment as shown in Scheme 1.4. β-Hydride elimination from the central carbon and migration to one of the terminal carbons yields a surface-bound propylene group, which can combine with a methylene group restarting the sequence of C-C bond formation. The Dry proposal is closely related to that by Maitlis in that the combination of "C_2" species with a methylene group is a pivotal step; in the Maitlis scheme, the C_2 species is an alkenyl group whereas it is an olefin in the Dry scheme.

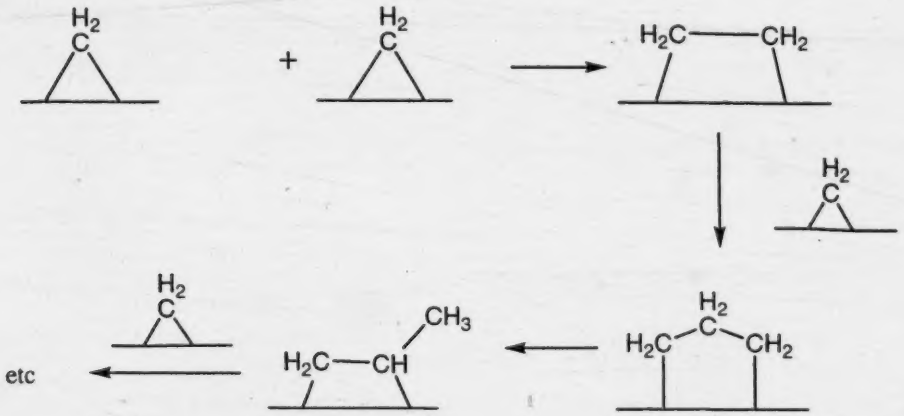

Scheme 1.4. *Dry scheme for methylene coupling and chain propagation.*

The metals from groups 8 (Fe, Ru, Os), 9 (Co, Rh, Ir) and 10 (Ni, Pd, Pt) are active as **FT** catalysts, although each metal yields a different distribution of products.[7] For example, ruthenium tends to give high molecular weight hydrocarbons, iron generally gives linear alkanes and oxygenates, cobalt yields linear alkanes, and rhodium primarily gives low molecular weight oxygenates and hydrocarbons. Although Ru is the most active **FT** catalyst, its expense dictates that it is not employed commercially; instead, inexpensive iron and cobalt are used. Even though cobalt catalysts generally have the longest industrial lifetime,[8] iron catalysts are more commonly employed because of their low cost. The selectivity shown by the different metal catalysts and the success of bimetallic catalysts in other important processes[9] suggests that bimetallic catalysts might also be promising in **FT** chemistry. Some **FT** mixed-metal systems have been shown to cooperatively change selectivity, thus altering the product distribution profiles.[10] A few reports have already appeared in which improved performance was observed using mixed Ru/Co catalysts in **FT** and related chemistry.[11]

The study of such mixed-metal, heterogeneous catalysts is largely empirical, and currently, little is understood about the roles of the different metals in this chemistry. The goals of our research are to synthesize metal complexes containing different combinations of metals from groups 8 and 9 and to study a series of carbon-carbon bond-forming reactions of relevance to **FT** chemistry. Through these model studies, an improved understanding of the functions of different metals in mixed-metal homogeneous systems will be obtained, which we hope will lead to a better understanding of related heterogeneous bimetallic **FT** catalysts. To date, mixed-metal systems based on the Ir/Ru,[12] Rh/Ru,[13] and Rh/Os[14] combinations of metals have been

investigated as models for **FT** chemistry, the last of which has been shown to be the most promising.

Initial studies into the carbon-carbon coupling of the Rh/Os system have been reported.[14] It was shown that the $[RhOs(CO)_4(dppm)_2][X]$ (**1.1** X= BF_4^-, $CF_3SO_3^-$) complexes have the ability to couple up to four "CH_2" fragments depending on the temperature at which the reaction is carried out as shown in Scheme 1.5. On the basis of

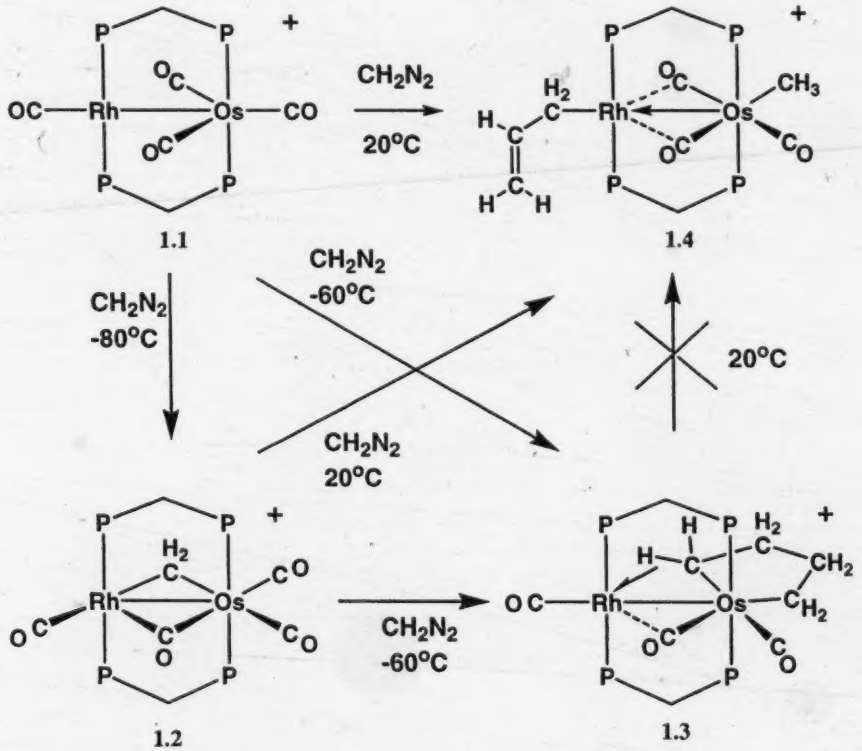

Scheme 1.5. *Reactivity of compound 1.1 with diazomethane.*

labelling studies, a mechanism has been proposed for the formation of both the butanediyl (**1.3**) and the allyl methyl (**1.4**) products from the methylene-bridged complex

(**1.2**). Stepwise insertion of diazomethane-generated methylene groups into the Rh-CH_2 bonds of the methylene-bridged **1.2** is proposed to give the putative ethylene-bridged **A** (see Scheme 1.6) followed by the propanediyl-bridged **C**. If additional methylene insertion occurs, the butanediyl product **1.3** results. At higher temperatures, β-hydrogen elimination from **C** becomes favourable and is proposed to yield the allyl hydride species (**D**), which upon reaction with diazomethane yields the allyl methyl product **1.4**. Clearly, the putative propanediyl-bridged intermediate (**C**) is a pivotal species in these transformations, leading to either the C_3 or C_4 fragment.

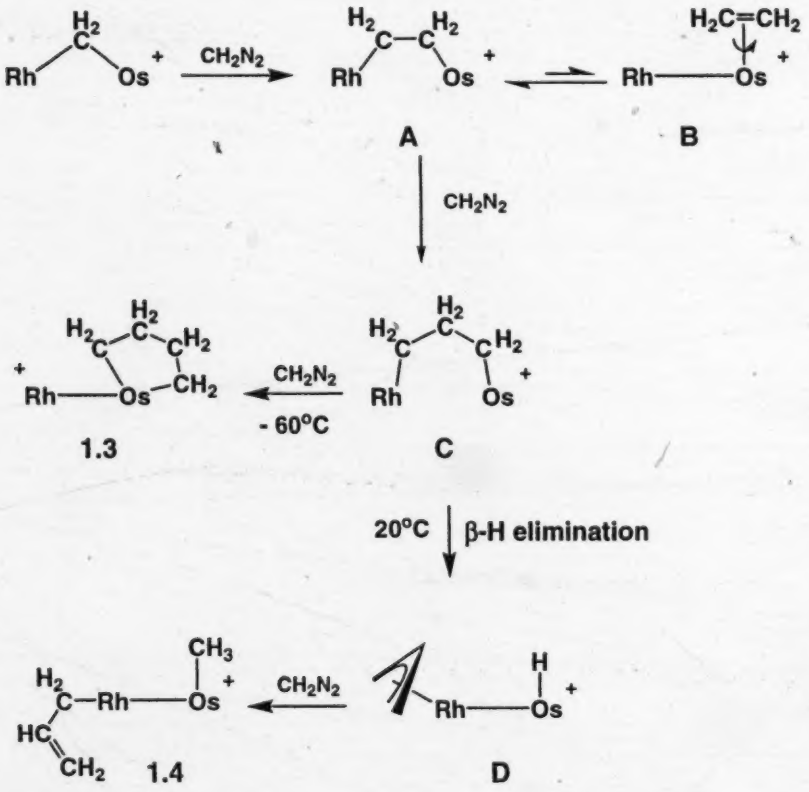

Scheme 1.6. *Mechanism for the formation of compounds **1.3** and **1.4**. All other ligands, apart from the hydrocarbyl groups are omitted for clarity.*

We therefore sought to investigate related C_3-bridged species. In our proposed mechanism rationalizing the formation of products **1.3** and **1.4**, the C_3 intermediate was proposed to result from CH_2 insertion into the Rh-C bond of an ethylene-bridged intermediate (Scheme 1.6). Thus, it would be expected that olefin insertion into the Rh-C bond of a bridging methylene species such as **1.2** should also give rise to C_3 species. Unfortunately, compound **1.2** proved to be unreactive towards olefins substrates.[15] Apart from their lack of reactivity with **1.2**, another problem relating to potential olefin reactions with a methylene-bridged species is products containing β-hydrogens might be susceptible to β-H elimination, preventing their isolation or even their observation. In order to be able to isolate the model C_3 species, it was felt necessary to eliminate the β-hydrogen decomposition pathway, leading us to consider substrates that would yield C_3-bridged moieties, but which did not have β-hydrogens. Based on this, alkynes and allenes seemed to be promising substrates.

Alkynes are able to interact with a pair of metals in a number of different ways; not only can the alkyne bind to only one of the metals, as observed in $[Ir_2(CO)_2(\eta^2\text{-}(F_3C)C{=}C(CF_3))(\mu\text{-}S)(\mu\text{-}CO)(dppm)_2]^+$,[16] it can also bridge the metals as is more commonly observed.[17] In a binuclear complex it is the bridging mode that is of interest since the potential of bridging ligand modes is what differentiates binuclear complexes from mononuclear ones. Furthermore, the bridging alkyne can bind in two ways, either parallel to the metals, in which case it functions as a 2-electron donor, or perpendicular to the metals, functioning as a 4-electron donor (Figure 1.1). Examples of both binding modes, shown in Figure 1.1, have been seen extensively throughout the literature of bimetallic systems.[18]

The reactions of terminal alkynes (HC≡CR) with bimetallic systems have been shown to proceed readily[17-19] to yield C_2-species. Puddephatt *et al.*[19a,c,d] have reported the

Figure 1.1. *Perpendicular and parallel alkyne binding modes in bimetallic systems.*

synthesis of a diruthenium complex, $[Ru(CO)_4(\mu\text{-}CO)(dppm)_2]$, which reacts with simple alkynes to give the alkyne-bridged product (Figure 1.2), in which the alkyne lies parallel to the metal-metal bond, forming a dimetallocyclobutene moiety. As outlined in Scheme 1.6, the second step in the methylene-coupling mechanism is postulated to yield a

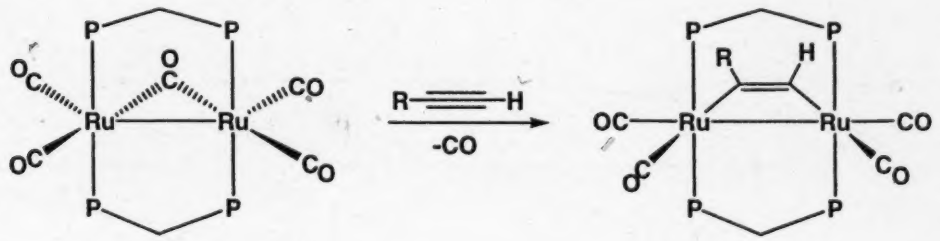

Figure 1.2. *Example of an alkyne-bridged dimetallic system.*

C_2-bridged ethylene intermediate (**A**), which subsequently reacts with diazomethane to generate the C_3H_6-bridged intermediate (**C**), which we are trying to model. The alkyne-bridged compounds are quite similar to the proposed intermediate **A**, and thus represents

a potentially robust species that can be used to model C_2-bridged intermediates to be used to subsequently build larger C_n frameworks.

Knox and co-workers have also studied the reaction of diruthenium systems with terminal alkynes such as phenylacetylene. In their work, the alkyne is found to react with the compound $[Ru_2(CO)_2(\mu\text{-}CO)_2(\eta^5\text{-}C_5H_5)_2]$ yielding the C_3 species $[Ru_2(CO)(\mu\text{-}CO)(\mu\text{-}\eta^1\text{:}\eta^3\text{-}C(O)CPhCPh)$.[20] This C_3 species bears a resemblance to the C_3H_6 intermediate proposed by Dry as illustrated in Scheme 1.4, except that in this case the hydrocarbyl fragment is formally a four-electron donor instead of a two-electron donor. In model systems, described though this thesis, the carbon atoms in the substituents bonded to core atoms are not counted in determining the "C_n" description. So, for example, the phenyl groups in the previous compound do not count since they model hydrogens in **FT** chemistry. The formation of other C_3-species has been seen through the reaction of bridging methylene groups and alkynes, a process that more closely resembles a step in **FT** chemistry. For example, in the reaction of the diiron, methylene-bridged compound, $Fe_2(\mu\text{-}CH_2)(CO)_8$, with acetylene, the C_3 species, $Fe_2(CO)_7(\mu,\eta^1\text{:}\eta^3\text{-}CHCHCH_2)$ results, as shown in Figure 1.3.[21] Again, in this example, the hydrocarbyl fragment functions as a four-electron donor to the metals, and can more appropriately be categorized as a vinyl carbene. These types of C_3-bridged compounds have been seen in a related dirhodium

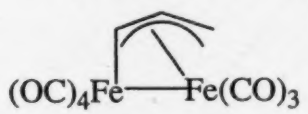

Figure 1.3. *A C_3-bridged dimetallic system.*

system reported by Maitlis *et al.*[22] Here, the addition of phenylacetylene to a "Rh(μ-CH_2)$_2$Rh" framework creates an insertion product in which the alkyne again donates 4 electrons to the metal centres. Addition of additional alkyne results in insertion into the remaining methylene bridge, and a head-to-tail dimerization of the alkyne (Scheme 1.7).

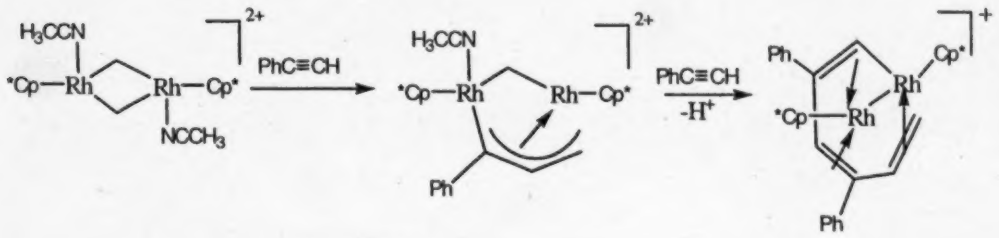

Scheme 1.7. *The dimerization of phenylacetylene through insertion into a (μ-CH_2) group.*

The reaction of allenes with mononuclear transition metal complexes has also been known to give C_3 products with insertion into a metal-carbon bond.[23] The reaction of substituted allenes with Pt[23a] and Pd[23b] complexes have shown that allenes readily insert into metal-alkyl and metal-aryl bonds. Allenes can also potentially yield C_3-bridged products through reaction with methylene-bridged precursors. We can envision two ways in which allenes could insert into a metal-carbon bond to yield C_3-bridged species similar to **C** shown earlier in Scheme 1.6. For substituted allenes, we assume that coordination to the metal via the unsubstituted double bond will occur due to lower steric hinderance, and in this case the two possibilities are diagrammed in Scheme 1.8. Species **F** is very similar to putative intermediates in insertion reactions involving ethylene and methylene groups, and as such contains β-hydrogen atoms and is susceptible to β-

hydrogen elimination. Species **E**, on the other hand, does not contain β-hydrogen atoms and may display greater stability.

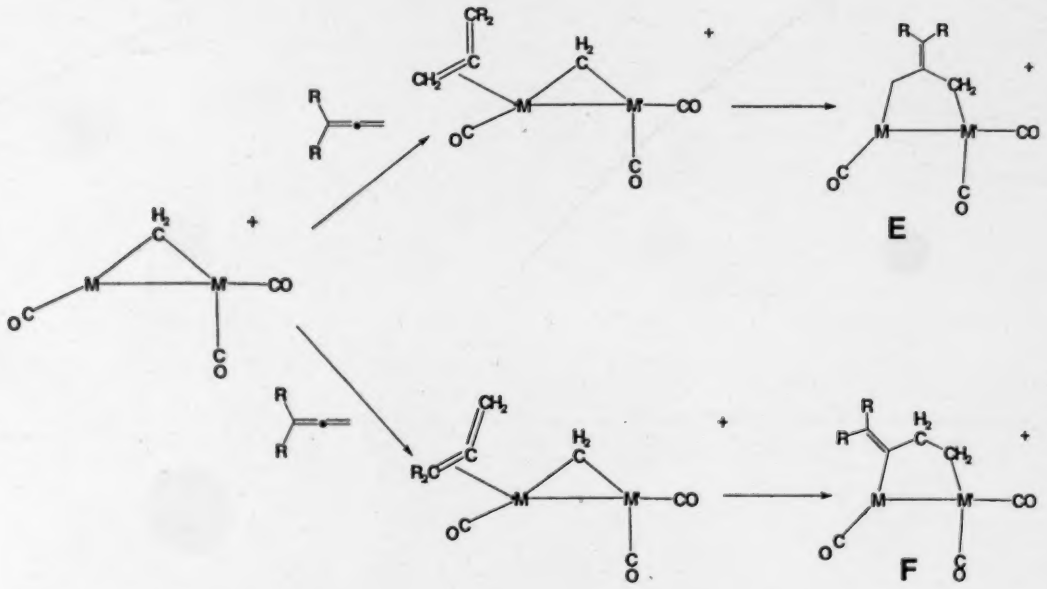

Scheme 1.8. *Possible isomers from allene insertion into a methylene unit.*

The framework of the bimetallic systems commonly studied in the Cowie group is an "A-frame" complex with two bridging dppm groups (dppm= *bis*-(diphenylphosphino)-methane), with additional ligands (L, L') on each of the metal centres, as shown in Figure 1.4. We have used the diphosphine ligand dppm (Figure 1.4) to hold the metals in close proximity in order to assure that the metals remain together during the chemistry of interest, and therefore have the potential to interact with substrate molecules in a cooperative manner. The strong metal-phosphorus bonds of late-metal complexes create a stable framework for the study of reactions with various

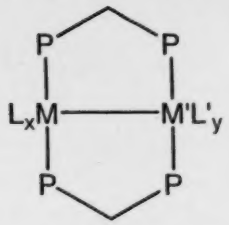

= $Ph_2PCH_2PPh_2$

M = Rh, Ir

M' = Ru, Os

Figure 1.4. *The framework of generic dppm-bridged A-frame complexes.*

organic substrates. In addition, the presence of NMR active ^{1}H and ^{31}P nuclei in this ligand, as well as the ^{1}H and ^{13}C nuclei in the other ligands of the complexes, are of immense importance to the characterization of these complexes. Although a wide variety of auxiliary ligands (L and L') can be used, we will emphasize the use of groups such as hydride, carbonyl or hydrocarbyl moieties, which are relevant in **FT** chemistry.

Our investigations into the chemistry of group 8/9 combinations of metals began with the Rh/Os combination since our research group already had extensive experience with these complexes, and the preparations of the precursor compounds were well-established.[24] The synthetic overview for the formation of Rh/Os complexes containing the desired framework involves the reaction of $[PPN][HOs(CO)_4]$ (PPN= bis(triphenylphosphoranylidene)ammonium) with $[RhCl(dppm)_2]$ as shown in Equation 2. Displacement of the chloride ligand, by the anionic osmium complex, is followed by unravelling of the chelating rhodium-bound dppm ligands into a bridging position on both metals to give the heterobinuclear complex $[RhOs(H)(CO)_3(dppm)_2]$. Transformation of this hydrido complex into the precursor complexes

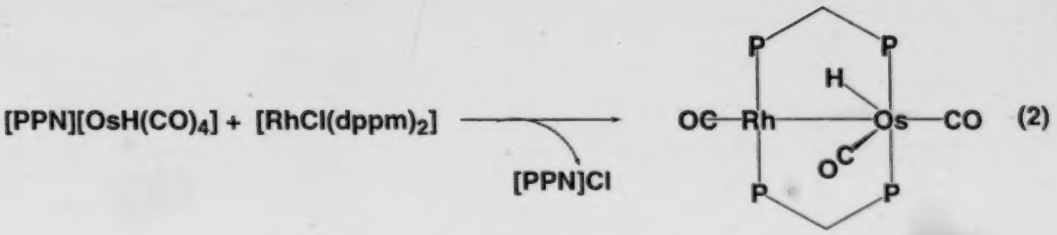

(2)

$[RhOs(CO)_4(dppm)_2][X]$ and $[RhOs(CO)_4(\mu\text{-}CH_2)(dppm)_2][X]$ ($X = BF_4^-$, $CF_3SO_3^-$) used in this thesis is well documented.[14,24]

In this thesis, we seek to generate model C_2-bridged and C_3-bridged complexes using alkynes and allenes as C_2 fragments and diazomethane-generated methylene groups as C_1 fragments. We will attempt to induce a stepwise formation of products containing higher order hydrocarbyl fragments by combination of the C_1 and C_2 fragments. This may lead to a better understanding of the types of carbon-carbon bond-forming reactions that can occur on metal surfaces and the roles of the different metals in the transformations.

References and Notes

1. (a) Huheey, J.E.; Keiter, E.A.; Keiter, R.L. *Inorganic Chemistry– Principles of Structure and Reactivity 4th Ed.* HarperCollins College Publishers: New York, **1993**. pp. 705-723. (b) Collman, J.P.; Hegedus, L.S.; Norton, J.R.; Finke, R.G. *Principles and Applications of Organotransition Metal Chemistry*, University Science Books: Mill Valley California, **1987**, pp. 523-660.

2. Schulz, H. *Appl. Cat. A.* **1999**, *186*, 3.

3. (a) Biloen, R.; Sachtler, W.M.H. *Adv. Catal.* **1981**, *30*, 165. (b) Fischer, F.; Tropsch, H. *Brennst. Chem.* **1926**, *7*, 97. (c) Brady, R.C.; Pettit, R. *J. Am. Chem. Soc.* **1981**, *103*, 1287. (d) Brady, R.C.; Pettit, R. *J. Am. Chem. Soc.* **1980**, *102*, 6181. (e) Gibson, V.C.; Parkin, G.; and Bercaw, J.E. *Organometallics* **1991**, *10*, 220.

4. Maitlis, P.M.; Long, H.C.; Quyoum, R.; Turner, M.L.; Wang, Z-Q. *Chem. Commun.* **1996**, 1.

5. (a) Isobe, K.; Andrews, D.G.; Mann, B.E.; Maitlis, P.M. *J. Chem. Soc. Chem. Commun.* **1981**, 809. (b) Maitlis, P.M.; Saez, I.M.; Meanwell, N.J.; Isobe, K.; Nutton, A.; Vaquez de Miguel, A.; Bruce, D.W.; Okeya, S.; Bailey, P.M.; Andrews, D.G.; Ashton, P.R.; Johnstone, I.R.; *New J. Chem,* **1989**, *13*, 419. (c) Turner, M.L.; Long, H.C.; Shenton, A.; Byers, P.K.; Maitlis, P.M. *Chem. Eur. J.* **1995**, *1*, 549. (d) Turner, M.L.; Byers, P.K.; Long, H.C.; Maitlis, P.M. *J. Am. Chem. Soc.* **1993**, *115*, 4417. (e) Long, H.C.; Turner, M.L.; Fornasiero, P.; Kăspar, J.; Graziani, M.; Maitlis, P.M. *J. Catal.* **1997**, *167*, 172.

6. Dry, M.E. *Appl. Catal. A.: General* **1996**, *138*, 319.

7. Bowker, M. *Catal. Today.* **1992**, *15*, 77.

8. Chaumette, P.; Courty P.; Kiennemann, A.; Ernst, B.; *Top. Cata.* **1995**, *2*, 117

9. Sinfelt, J.H. *Bimetallic Catalysts*, John Wiley & Sons, New York, NY, **1983**.

10. (a) Sun, S.; Fujimoto, K.; Yoneyama, Y.; Tsubaki, N. *Fuel* **2002**, *81*, 1583. (b) Tsubaki,N.; Sun, S.L.; Fujimoto, K. *J. Mol. Catal.* **2001**, *199*, 236. (c) Kariya, N.; Fukuoka, A.; Ichikawa, M. *Appl. Catal. A* **2002**, *233*, 91. (d) Maunula, T.; Ahola, J.; Salmi, T.; Haario, H.; Harkonen, M.; Luoma, M.; Pohjola, V.J. *Appl. Catal. B* **1997**, *12*, 287. (e) Adesina, A.A. *Appl. Catal. A* **1996**, *138*, 345.

11. (a) Huang, L.; Xu, Y. *Catalysis Letters.* **2000**, *69*, 145. (b) Xiao, F.-S.; Ichikawa, M. *J. Catal.* **1994**, *147*, 304.

12. Dell' Anna, M.M.; Trepanier, S.J.; McDonald, R.; Cowie, M. *Organometallics* **2001**, *20*, 88.

13. Rowsell, B.D.; Trepanier, S.J.; Lam, R.; McDonald, R.; Cowie, M. *Organometallics* **2002**, *21*, 3228.

14. Trepanier, S.J.; Sterenberg, B.T.; McDonald R.; Cowie, M. *J. Am. Chem. Soc.* **1999**, *121*, 2613.

15. Trepanier, S.J., Ph.D. Thesis, University of Alberta, Edmonton, Alberta, **2002**.

16. Vaartstra, B.A.; Cowie, M. *Organometallics,* **1989**, *8*, 2388.

17. Rowsell, B.D.; McDonald, R.; Ferguson, M.J.; Cowie, M. *Organometallics* **2003**, *22*, 2944. (b) Torkelson, J.R.; McDonald, R.; Cowie, M.. *Organometallics* **1999**, *18*, 4134. (c) George, D.S.A.; McDonald, R.; Cowie, M. *Organometallics* **1998**, *17*, 2553.

18. (a) Hoffman, D.M.; Hoffmann, R.; Fisel, C.R. *J. Am. Chem. Soc.* **1982,** *104*, 3858. (b) McKeer, I.R.; Sherlock, S.J.; Cowie, M. *J. Organomet. Chem.* **1988,** *352*, 205. (c) Mague, J.T. *Organometallics* **1986,** *5*, 918. (d) Dickson, R.S.; Pain, G.N. *J. Chem.Soc.*,

Chem. Commun. **1979**, 277. (e) Berry, D.H.; Eisenberg, R. *Organometallics* **1987,** *6,* 1796.

19. (a) Puddephatt, R.J.; Vittal, J.J.; Mirza, H.A.; Kuncheria, J. *Inorg. Chem.Comm.* **1999**, *2*, 197. (b) Gladfelter W.L.; Johnson, K.A.; *Organometallics* **1992**, *11*, 2534. (c) Thomson, M.A.; Puddephatt, R.J. *Inorg. Chem.* **1982**, *21*, 725. (d) Thomson, M.A.; Puddephatt, R.J. *Inorg. Chim. Acta.* **1980**, *45*, L281. (e) Cowie, M.; Mague, J.T.; Sanger, A.R. *J. Am. Chem. Soc.* **1978**, *100*, 3628.

20. Dyke, A.F.; Knox, S.A.R.; Naish, P.J.; Taylor, G.E. *J. Chem. Soc. Dalton Trans.* **1982**, 1297.

21. Sumner, C.E., Jr.; Collier, J.A.; Pettit, R. *Organometallics* **1982**, *1*, 1350.

22. Kaneko, Y.; Suzuki, T.; Isobe, K.; Maitlis, P.M. *J. Organometal. Chem.* **1998**, *554*, 155.

23. (a) Yagyu, T.; Suzaki, Y.; Osakada, K. *Organometallics* **2001**, *21*, 2088. (b) Canovese, L.; Visentin, F.; Chessa, G.; Uguagliati, P; Bandoli, G. *Organometallics* **2000**, *19*, 1461.

24. (a) Antonelli, D. M.; Cowie, M. *Organometallics* **1990**, *9*, 1818. (b) Hilts, R.; Franchuk, R.; Cowie, M. *Organometallics* **1991**, *10*, 304.

Chapter 2.

Formation of C_3 and C_4 Species Through Coupling of Alkynes and Methylene Groups.

Introduction

As stated in Chapter 1, there has been recent interest in bimetallic Fischer-Tropsch (**FT**) chemistry. The Cowie group has been investigating the chemistry of bimetallic compounds of the group 8/9 metals,[1] and have previously reported the ability of $[RhOs(CO)_4(dppm)_2][CF_3SO_3]$ (**1.1**) to couple up to four methylene units.[1b] The reaction of compound **1.1** with diazomethane at –80°C yielded the methylene-bridged compound $[RhOs(CO)_4(\mu\text{-}CH_2)(dppm)_2][CF_3SO_3]$ (**1.2**) which transformed into the unusual C_4-containing product, $[RhOs(CO)_3(C_4H_8)(dppm)_2][CF_3SO_3]$ (**1.3**), in the presence of excess diazomethane at somewhat higher temperatures (-40 to -60°C) and into the allyl methyl complex, $[RhOs(CO)_3(\eta^1\text{-}C_3H_3)(CH_3)(dppm)_2]^+$ (**1.4**) at ambient temperature. No C_2 or C_3 intermediates were observed in these transformations.

Dry has proposed that a C_3H_6-bridged intermediate is an important species in the chain-propagation step of the **FT** process.[2] This work has attempted to model these C_2- and C_3-bridged intermediates and the stepwise transformations between C_2, C_3, and C_4 products through the use of alkynes as C_2 modules and methylene groups as C_1 fragments. Two approaches will be investigated toward the preparation of model C_3-bridged products, involving either reaction of the methylene-bridged complex, $[RhOs(CO)_4(\mu\text{-}CH_2)(dppm)_2][X]$ (**1.2**)[1b] or realated species with alkynes, or reactions of the alkyne-bridged $[RhOs(CO)_3(\mu\text{-}RC{=}CR)(dppm)_2][X]$ (R= CO_2CH_3 (**2.8**) R= CF_3 (**2.9**)) with methylene groups.

Experimental Section

General Comments. All solvents were dried using the appropriate desiccants, distilled before use and stored under argon. Reactions were carried out under an argon atmosphere using standard Schlenk techniques. Diazomethane was produced from Diazald, purchased from Aldrich, as was dimethyl acetylenedicarboxylate (DMAD) and hexafluoro-2-butyne (HFB). ^{13}C-Diazald was purchased from Cambridge Isotope Laboratory and ^{13}CO (99 % enriched) was purchased from Isotech, Inc. The complexes $[RhOs(CO)_4(\mu\text{-}CH_2)(dppm)_2][CF_3SO_3]$ (**1.2**),[1b] $[RhOs(CO)_3(\mu\text{-}CH_2)(dppm)_2][CF_3SO_3]$ (**2.1**)[3] $[RhOs(CO)_3(\mu\text{-}(CO_2CH_3)C{=}C(CO_2CH_3))(dppm)_2][CF_3SO_3]$ (**2.8**),[4] and $[RhOs(CO)_3(\mu\text{-}(F_3C)C{=}C(CF_3)(dppm)_2][CF_3SO_3]$ (**2.9**)[4] were prepared by the published procedures.

The ^{1}H, ^{13}C{^{1}H}, ^{1}H-^{1}H COSY, and ^{31}P{^{1}H} NMR spectra were recorded on a Varian iNova-400 spectrometer operating at 399.8 MHz for ^{1}H, 161.8 MHz for ^{31}P{^{1}H} and 100.6 MHz for ^{13}C{^{1}H}. Infrared spectra were obtained on a Nicolet Magna 750 FTIR spectrometer with a NIC-Plan IR microscope. The elemental analyses were performed by the microanalytical service within the department. Electrspray ionization mass spectra were run on a Micromass ZabSpec spectrometer by the staff in the Mass Spectrometry Services Laboratory. In all cases, the distribution of isotope peaks for the appropriate parent ion matched that calculated for the formula given.

Preparation of Compounds

(a) **$[RhOs(CO)_3(\mu\text{-}\eta^1\text{:}\eta^1\text{-}(CO_2CH_3)C{=}C(CO_2CH_3)CH_2)(dppm)_2][CF_3SO_3]$ (2.2).** 62.8 mg (0.0480 mmol) of **2.1** was dissolved in 5 mL of CH_2Cl_2, and excess dimethyl acetylenedicarboxylate (DMAD) (33.6 μL, 0.274 mmol, 6 equiv) was added, resulting in an immediate colour change from red to yellow. The solution was stirred for 30 minutes, a yellow residue was precipitated by the addition of 15 mL of diethyl ether and 30 mL of pentane, followed by filtration and drying of the solid *in vacuo* (yield 84%). Anal. Calcd. for $C_{61}H_{52}O_{10}F_3P_4RhOsS$: C, 50.49; H, 3.61. Found: C, 50.12; H, 3.52. MS: *m/z* 1303 ($M^+ - CF_3SO_3^-$).

(b) **$[RhOs(CO)_3(\mu\text{-}\eta^1\text{:}\eta^1\text{-}(CF_3)C{=}C(CF_3)CH_2)(dppm)_2][CF_3SO_3]$ (2.3).** Hexafluoro-2-butyne (HFB) was slowly passed, at a rate of 2 mL/min for 5 minutes, through a solution of compound **2.1** (118mg, 0.090 mmol) in 10 mL of CH_2Cl_2 for 5 minutes resulting in a rapid colour change from red to yellow. The solution was stirred for 30 minutes, followed by the precipitation of a yellow solid by the addition of 15 mL of diethyl ether followed by 30 mL of pentane. The solid was filtered and dried under a stream of argon (yield 82%). Anal. Calcd. for $C_{59}H_{46}F_9O_6P_4RhOsS$: C, 49.49; H, 3.29. Found: C, 48.89; H, 3.11. MS: *m/z* 1323 ($M^+ - CF_3SO_3^-$).

(c) **$[RhOs(CF_3SO_3)(CO)_2(\mu,\eta^1\text{:}\eta^1\text{-}(CO_2CH_3)C{=}C(CO_2CH_3)CH_2)(dppm)_2]$ (2.4).** 5 mL of CH_2Cl_2 was added to a mixture of 40 mg (0.025 mmol) of compound **2.2** and 2.0 mg (0.027 mmol) of Me_3NO, resulting in a rapid colour change from yellow to orange. The solution was stirred for 20 minutes, and a red solid was precipitated using 15 mL of diethyl ether followed by 30 mL of pentane. The solid was filtered and dried under a stream of argon (yield 77%). MS: *m/z* 1275 ($M^+ - CF_3SO_3^-$).

Table 2.1. Spectroscopic Data For Compounds.

Compound	IR (cm^{-1})[a, b]	NMR[d,e] $^{31}P\{^1H\}$ (ppm)[f]	NMR[d,e] ^1H (ppm)[g, h]	NMR[d,e] $^{13}C\{^1H\}$ (ppm)[h, i]
$[RhOs(CO)_3(\mu\text{-}\eta^1\text{:}\eta^1\text{-}(CO_2CH_3)C{=}C(CO_2CH_3)\text{-}CH_2)(dppm)_2][CF_3SO_3]$ (**2.2**)	2030 (s), 2009 (s), 1936 (m), 1702 (br, m)	26.6 (dm. $^1J_{RhP}$= 113Hz), -1.5 (m)	4.67 (m, 2H, dppm), 3.94 (m, 2H, dppm), 3.17 (s, 3H), 2.71 (s, 3H), 1.68 (br, t, 2H, CH_2)	191.3 (dt, $^2J_{PC}$ = 12 Hz, $^1J_{RhC}$= 51 Hz, 1C), 183.7 (t, $^2J_{PC}$ = 11 Hz, 1C), 171.4 (t, $^2J_{PC}$ = 12 Hz, 1C), 7.7 (t, $^2J_{PC}$ = 7 Hz, 1C)
$[RhOs(CO)_3(\mu\text{-}\eta^1\text{:}\eta^1\text{-}(CF_3)C{=}C\text{-}(CF_3)CH_2)(dppm)_2][CF_3SO_3]$ (**2.3**)	2037 (s), 2010 (br, m) 1945 (s)	24.0 (dm, $^1J_{RhP}$= 105Hz), -3.2(m)	4.21 (m, 2H, dppm), 4.12 (m, 2H, dppm), 2.00 (m, 2H, CH_2)	194.0 (m, 1C), 193.1 (t, $^2J_{PC}$ = 14 Hz, 1C), 191.3 (dt, $^2J_{PC}$ = 12 Hz, $^1J_{RhC}$ = 50 Hz, 1C), 13.8 (t, $^2J_{PC}$ = 8 Hz, 1C)
$[RhOs(CF_3SO_3)(CO)_2(\mu\text{-}\eta^1\text{:}\eta^1\text{-}(CO_2CH_3)C{=}C\text{-}(CO_2CH_3)CH_2)(dppm)_2][CF_3SO_3]$ (**2.4**)	2012 (s), 1908 (s)	28.8 (br), -4.6 (br)	4.34 (m, 4H, dppm), 3.36 (s, 3H, OMe), 1.29 (s, 3H, OMe), 1.06 (t, 2H, CH_2, $^1J_{CH}$= 128 Hz)	-3.5 ($^1J_{CH}$= 130, $^2J_{PC}$= 10 Hz)

Table 2.1. Spectroscopic Data For Compounds (cont'd).

		NMR[d,e]		
Compound	IR (cm^{-1})[a, b]	$^{31}P\{^{1}H\}$ (ppm)[f]	^{1}H (ppm)[g, h]	$^{13}C\{^{1}H\}$ (ppm)[h, i]
$[RhOs(CF_3SO_3)(CO)_2(\mu\text{-}\eta^1\text{:}\eta^1\text{-}CF_3)C{=}C(CF_3)CH_2)\text{-}(dppm)_2][CF_3SO_3]$ (**2.5**)		25.8 (br), -5.1 (m)	4.48 (m, 2H, dppm), 3.92 (m, 2H, dppm), 1.63 (br, 2H)	
$[RhOs(CO)_3(\mu\text{-}\eta^1\text{:}\eta^1\text{-}CH_2(CO_2Me)C{=}C\text{-}(CO_2Me)CH)(\mu\text{-}H)(dppm)_2]\text{-}[CF_3SO_3]$ (**2.7**)	2056(m), 2031 (s), 1976 (m), 1691 (br, m), 1578 (m)[j]	24.3 (dm, $^{1}J_{RhP}$= 99Hz)), -8.8 (m)	5.29 (dt, 1H, $^{2}J_{RhH}$= 2 Hz, $^{3}J_{PH}$= 4 Hz, $^{1}J_{CH}$= 161 Hz, μ-CH), 5.14 (m, 2H, $^{1}J_{PH}$= 4 Hz, dppm), 4.32 (m, 2H, $^{1}J_{PH}$= 4 Hz, dppm), 4.07 (dt, 2H, $^{2}J_{RhH}$ = 2 Hz, $^{3}J_{PH}$= 11 Hz, CH_2), 3.92 (s, 3H, OMe), 3.05 (s, 3H, OMe)	188.2 (dt, $^{2}J_{PC}$ = 12 Hz, $^{1}J_{RhC}$= 46Hz, 1C), 185.0(t, $^{2}J_{PC}$ = 11 Hz, 1C) 176.7(t, $^{2}J_{PC}$ = 11 Hz, 1C), 118.3 (d, $^{2}J_{RhC}$= 16 Hz, 1C, μ-CH), 70.3 (br, d, $^{1}J_{RhC}$= 25 Hz, 1C, CH_2)

Table 2.1. Spectroscopic Data For Compounds (cont'd).

Compound	IR (cm^{-1})[a, b]	NMR[d,e] $^{31}P\{^1H\}$ (ppm)[f]	^1H (ppm)[g, h]	$^{13}C\{^1H\}$ (ppm)[h, i]
$[RhOs(CO)_3(\mu\text{-}\eta^1\text{:}\eta^1\text{-}CH_2(CO_2CH_3)C{=}C(CO_2CH_3)(dppm)_2][BF_4]$ (**2.10**)[g]		19.6 (dm, $^1J_{RhP}$= 160Hz), -17.9 (m)	4.82 (m, 2H, CH_2, $^1J_{CH}$= 152 Hz), 4.26 (m, 2H, dppm), 4.08 (m, 2H, dppm),	200.4 (dt, 1C, $^1J_{RhC}$= 49Hz, $^2J_{PC}$= 14Hz), 192.9 (m, 1C), 178.6 (s, 1C), 176.6 (t, 1C, $^2J_{PC}$= 9Hz), 100.5 ($^1J_{RhC}$= 28 Hz),
$[RhOs(CO)_3(\mu\text{-}\eta^1\text{:}\eta^1\text{-}C(CO_2CH_3){=}C(CO_2CH_3)(\mu\text{-}CH_2)(dppm)_2][BF_4]$ (**2.11**)	1996 (m), 1949 (br, sh)	32.3 (dm, $^1J_{RhP}$= 113 Hz), 0.6 (m)	4.01 (m, 2H, dppm), 3.89 (m, 2H, dppm), 3.72 (s, 3H, OMe), 2.10 (s, 3H, OMe), 1.32 (m, 2H, $^1J_{CH}$= 128 Hz, CH_2)	190.8 (dt, 1C, $^1J_{RhC}$= 52 Hz, $^2J_{PC}$= 12Hz), 190.7 (m, 1C, Os(CO), 169.6 (m, 1C, Os(CO), 30.6 (μ-CH_2, 1C, J_{RhC}= 33Hz, J_{PC}= 13Hz)

[a] IR abbreviations: s = strong, m = medium, w = weak, sh = shoulder. [b] CH_2Cl_2 solutions unless otherwise stated, in units of cm^{-1}. [c] Carbonyl stretches unless otherwise noted. [d] NMR abbreviations: s = singlet, d = doublet, t = triplet, m = multiplet, dm = doublet of multiplets, om = overlapping multiplets, br = broad, dt = doublet of triplets. [e] NMR data at 25°C in CD_2Cl_2 unless otherwise stated. [f] ^{31}P chemical shifts referenced to external 85% H_3PO_4. [g] NMR data collected at 80°C in CD_2Cl_2. [h] Chemical shifts for the phenyl hydrogens are not given. [i] ^1H and ^{13}C chemical shifts referenced to TMS. [j] $^{13}C\{^1H\}$ NMR performed with ^{13}CO enrichment

(d) **[RhOs(CF_3SO_3)(CO)$_2$(μ,η^1:η^1-(CF_3)C=C(CF_3)CH_2)(dppm)$_2$] (2.5).** 5 mL of CH_2Cl_2 was added to a mixture of 36 mg (0.025 mmol) of compound **2.3** and 2 mg (0.027 mmol) of Me_3NO, resulting in a rapid colour change from yellow to orange. The solid was stirred for 20 minutes and precipitated by the slow addition of 20 mL of diethyl ether, followed by 40 mL of pentane. The solid was filtered and dried under a stream of argon (yield 76%). MS: *m/z* 1295 (M^+ - $CF_3SO_3^-$).

(e) **[RhOs(CO)$_3$(μ-η^1: η^1-$CH_2C(CO_2CH_3)$=C(CO_2CH_3)CH)(μ-H)(dppm)$_2$]-[CF_3SO_3] (2.7).** Diazomethane, generated from 50 mg of Diazald (0.23 mmol, 17 equiv) was vigorously passed through a 10 mL solution of compound **2.2** (50 mg, 0.014 mmol) in CH_2Cl_2, resulting in a colour change from yellow to orange. The residue was extracted using 15 mL of diethyl ether and 30 mL of pentane, and dried under a stream of argon (yield 86%). MS: *m/z* 1317 (M^+ - $CF_3SO_3^-$).

(f) **Attempted reaction of 2.3 + CH_2N_2.** An excess of diazomethane (20mg, 0.094 mmol, 7 equiv) was bubbled through an NMR tube of compound **2.3** (20 mg, 0.014 mmol). The colour of the solution changed from yellow to orange over the course of one day, but only compound **2.3** was detected via $^{31}P\{^1H\}$ NMR spectroscopy.

(g) **[RhOs(CO)$_3$(μ-η^1:η^1-CH_2(CO_2Me)C=C(CO_2Me))(dppm)$_2$][CF_3SO_3] (2.10).** 50 mg (0.035 mmol) of compound **2.8** was dissolved in 15 ml of CH_2Cl_2 and cooled to -80°C. An excess of diazomethane generated from Diazald (50 mg, 0.23 mmol, 7 equiv) was vigorously passed through the solution, resulting in a rapid colour change from orange to green. Satisfactory elemental analyses for this compound could not be obtained since it was not stable at ambient or higher temperatures.

(h) $[RhOs(CO)_3(\mu\text{-}CH_2)(\mu\text{-}\eta^1{:}\eta^1\text{-}(CO_2Me)C{=}C(CO_2Me))(dppm)_2][CF_3SO_3]$ (2.11). An excess of diazomethane generated from Diazald (50 mg, 0.23 mmol, 7 equiv) was bubbled through a solution of 50 mg (0.034 mmol) of **2.10** in 10 mL of CH_2Cl_2 at -80°C. The solution was stirred at low temperature for 30 minutes. The excess diazomethane was removed by placing the sample under vacuum 30 minutes at 80°C, then the sample was gradually warmed to room temperature while under dynamic vacuum. As the solution warmed to ambient temperature, the solution colour changed from green to orange. The solid was isolated at ambient temperature by the slow addition of 15 mL of diethyl ether followed by 30 mL of pentane. The solid was filtered and then dried under a stream of argon (yield 72%).

(i) Reaction of 2.8 + CH_2N_2 at RT. Diazomethane generated from Diazald (50 mg, 0.23 mmol, 7 equiv) was bubbled through a solution of 50 mg of compound **2.8** dissolved in 10 mL of CH_2Cl_2, resulting in an immediate colour change from orange to yellow. The solution was stirred for 30 minutes, the solid was isolated using 10 ml of diethyl ether and 25 ml of pentane, and dried in vacuo.

(j) Reaction of 2.9 + CH_2N_2. An excess of diazomethane generated from Diazald (50 mg, 0.23 mmol, 17 equiv) was bubbled through 20 mg (0.014 mmol) of compound **2.9**.[4] A rapid colour change was observed from yellow to orange. NMR spectroscopy of the resultant solution showed a 1:1 mixture of compounds **2.3** and **1.2** based on NMR integration, with a variety of unidentifiable products.

X-ray Data Collection.

All X-ray crystallography was completed by Drs. Robert McDonald and Michael J. Ferguson of the Department of Chemistry X-ray Crystallography Services Facility at the University of Alberta.

(a) Pale yellow crystals of $[RhOs(CO)_3(\mu\text{-}\eta^1\text{:}\eta^1(COOCH_3)C{=}C(COOCH_3)CH_2)\text{-}(dppm)_2][CF_3SO_3]$ (**2.2**) were isolated from a solution of dichloromethane-d_2 via slow evaporation of the NMR sample. Data were collected on a Bruker PLATFORM/SMART 1000 CCD diffractometer[5] using Mo Kα radiation at –80°C. Unit cell parameters were obtained from a least-squares refinement of the setting angles of 11686 reflections from the data collection. The space group was determined to be P$\bar{1}$ based upon the diffraction symmetry, the lack of systematic absences and the successful refinement of the structure. The data were corrected for absorption through use of the SADABS procedure.

(b) Pale yellow crystals containing a 1:1 mixture of $[RhOs(CO)_3(\mu\text{-}\eta^1\text{:}\eta^1\text{–}(CF_3)C{=}C\text{-}(CF_3)CH_2)(dppm)_2][CF_3SO_3]$ (**2.3**) and $[RhOsCl(CO)_2(\mu\text{-}\eta^1\text{:}\eta^1\text{-}C(CF_3){=}C(CF_3)CH_2)\text{-}(dppm)_2]$ (**2.6**) were inadvertently co-crystallized from a solution in dichloromethane-d_2 via slow evaporation. Data were collected on a Bruker PLATFORM/SMART 1000 CCD diffractometer using Mo Kα radiation at –80°C. Unit cell parameters were obtained from a least-squares refinement of the setting angles of 9376 reflections from the data collection. The space group was determined to be $P2_1/n$ (a non-standard setting of $P2_1/c$ (No. 14)). The data were corrected for absorption through use of the SADABS procedure.

Structure Solution and Refinement

The structure of compound **2.2** was solved using direct methods (SHELXS-86).[6] Refinement was completed using the program SHELXL-93.[7] Hydrogen atoms were assigned positions based on the geometries of their attached carbon atoms, and were given thermal parameters 20% greater than those of the attached carbons.

The structures of compounds **2.3** and **2.6** were solved using the direct methods program SHELXS-86, and refinement was completed using the program SHELXL-93, during which the hydrogen atoms were treated as for compound **2.2**. Remaining atoms were located from the difference Fourier map of subsequent least-squares refinement. The single crystal of this sample was found to contain a 1:1 disordered mixture of compounds **2.3** and **2.6**. These molecules were found to have exactly the same orientations so that the only evidence for the presence of both compounds was the overlapping half-occupancy Cl and CO ligands on Rh. Clearly the triflate anion is also only present as half occupancy. Refinement of the structure proceeded well with all atoms behaving well. A solution of the solid showed the presence of only compound **2.3** via $^{31}P\{^{1}H\}$ NMR spectroscopy, indicating that only a small number of crystals contained the mixture of both compounds; it is assumed that the few suitable crystals have the disordered mixture of **2.3** and **2.6**, while the bulk of the sample, which does not crystallize suitably, is composed of compound **2.3**.

Results and Compound Characterization

The addition of the symmetrical alkynes DMAD and HFB to the methylene-bridged tetracarbonyl complex, $[RhOs(CO)_4(\mu\text{-}CH_2)(dppm)_2][CF_3SO_3]$ (**1.2**),[1b] does not

Table 2.2. Crystallographic Experimental Details for Compounds **2.2** and **2.6.**

Formula	$C_{65.5}H_{63}BCl_{11}F_4O_7OsP_4Rh$	$C_{59}H_{48}Cl_{2.50}F_{7.50}O_4OsP_4RhS_{0.50}$
formula weight	1855.91	1485.12
crystal dimensions (mm)	0.52 x 0.46 x 0.11	0.37 × 0.07 × 0.05
crystal system	triclinic	monoclinic
space group	$P\bar{1}$ (No. 2)	$P2_1/n$ (an alternate setting of $P2_1/c$ [No. 14])
unit cell parameters[a]		
a (Å)	12.458 (1)	12.3863 (8)
b (Å)	15.222 (2)	18.981 (1)
c (Å)	20.881 (2)	25.967 (2)
α (deg)	90.438 (2)	
β (deg)	92.241 (2)	97.086 (1)
γ (deg)	107.474 (2)	
V (Å^3)	3773.3 (7)	6058.2 (7)
Z	2	4
ρ_{calcd} (g cm^{-3})	1.633	1.628
μ (mm^{-1})	2.434	2.669
Data Collection and Refinement Conditions		
diffractometer	Bruker PLATFORM/SMART 1000 CCD[b]	Bruker PLATFORM/SMART 1000 CCD[b]

radiation (λ [Å])	graphite-monochromated Mo Kα (0.71073)	graphite-monochromated Mo Kα (0.71073)
temperature (°C)	–80	-80
scan type	ω scans (0.2°) (30 s exposures)	ω scans (0.2°) (25 s exposures)
data collection 2θ limit (deg)	52.92	52.76
total data collected	19250 ($-15 \le h \le 15$, $-18 \le k \le 19$, $-26 \le l \le 20$)	34347 ($-15 \le h \le 13$, $-22 \le k \le 23$, $-32 \le l \le 32$)
independent reflections	15127 (R_{int} = 0.0420)	12407 (R_{int} = 0.0560)
number of observed reflections (NO)	11686 [$F_o^2 \ge 2\sigma(F_o^2)$]	9376 [$F_o^2 \ge 2\sigma(F_o^2)$]
structure solution method	Patterson search/structure expansion (DIRDIF–96[c])	direct methods (*SHELXS–86*[d])
refinement method	full-matrix least-squares on F^2 (SHELXL–93[e])	full-matrix least-squares on F^2 (SHELXL–93[e])
absorption correction method	Gaussian integration (face-indexed)	empirical (*SADABS*)
range of transmission factors	0.7756–0.3642	0.8781–0.4384
data/restraints/parameters	15127 [$F_o^2 \ge -3\sigma(F_o^2)$] / 0 / 865	12407 [$F_o^2 \ge -3\sigma(F_o^2)$] / 25[f] / 711

goodness-of-fit (S)[g]	1.132 [$F_o^2 \geq -3\sigma(F_o^2)$]	1.046 [$F_o^2 \geq -3\sigma(F_o^2)$]
final R indices[h]		
R_1 [$F_o^2 \geq 2\sigma(F_o^2)$]	0.0735	0.0523
wR_2 [$F_o^2 \geq -3\sigma(F_o^2)$]	0.2007	0.1494
largest difference peak and hole	6.580 and –2.831 e Å^{-3}	2.739 and –1.572 e Å^{-3}

[a] Obtained from least-squares refinement of 5423 reflections for compound **2.2** and 4879 reflections for compound **2.6**

[b] Programs for diffractometer operation, data collection, data reduction and absorption correction were those supplied by Bruker.

[c] Beurskens, P. T.; Beurskens, G.; Bosman, W. P.; de Gelder, R.; Garcia Granda, S.; Gould, R. O.; Israel, R.; Smits, J. M. M. (1996). The *DIRDIF-96* program system. Crystallography Laboratory, University of Nijmegen, The Netherlands.

[d] Sheldrick, G. M. *Acta Crystallogr.* **1990**, *A46*, 467.

[e] Sheldrick, G. M. *SHELXL-93*. Program for crystal structure determination. University of Göttingen, Germany, 1993. Refinement on F_o^2 for all reflections (all of these having $F_o^2 \geq -3\sigma(F_o^2)$). Weighted R-factors wR_2 and all goodnesses of fit S are based on F_o^2; conventional R-factors R_1 are based on F_o, with F_o set to zero for negative F_o^2. The observed criterion of $F_o^2 > 2\sigma(F_o^2)$ is used only for calculating R_1, and is not relevant to the choice of reflections for refinement. R-factors based on F_o^2 are statistically

about twice as large as those based on F_o, and R-factors based on ALL data will be even larger.

[f] The S–O, S–C, C–F, O···O, F···F and O···F (excluding *trans*-O···F) distances of the triflate anion were restrained to be 1.45(1), 1.80(1), 1.35(1), 2.37(1), 2.20(1) and 3.04(1) Å, respectively. The C–Cl and Cl···Cl distances of the dichloromethane solvent molecules were restrained to be 1.80(1) and 2.95(1) Å, respectively.

[g] $S = [\Sigma w(F_o^2 - F_c^2)^2/(n - p)]^{1/2}$ (n = number of data; p = number of parameters varied; $w = [\sigma^2(F_o^2) + (0.0806P)^2 + 18.7082P]^{-1}$ where $P = [\mathrm{Max}(F_o^2, 0) + 2F_c^2]/3)$.

[h] $R1 = \Sigma||F_o| - |F_c||/\Sigma|F_o|$; $wR2 = [\Sigma w(F_o^2 - F_c^2)^2/\Sigma w(F_o^4)]^{1/2}$.

proceed under ambient conditions. However, the removal of a carbonyl from compound **1.2** through the use of trimethylamine N-oxide yields the highly reactive tricarbonyl complex, $[RhOs(CO)_3(\mu\text{-}CH_2)(dppm)_2][CF_3SO_3]$ (**2.1**),[3] which reacts instantly with these alkynes to form the two new species $[RhOs(CO)_3(\mu\text{-}\eta^1\text{:}\eta^1\text{-}(CO_2CH_3)C{=}C(CO_2CH_3)CH_2)\text{-}(dppm)_2][CF_3SO_3]$ (**2.2**) and $[RhOs(CO)_3(\mu\text{-}\eta^1\text{:}\eta^1\text{-}(CF_3)C{=}C(CF_3)CH_2)(dppm)_2][CF_3SO_3]$ (**2.3**) respectively, as shown in Scheme 2.1.

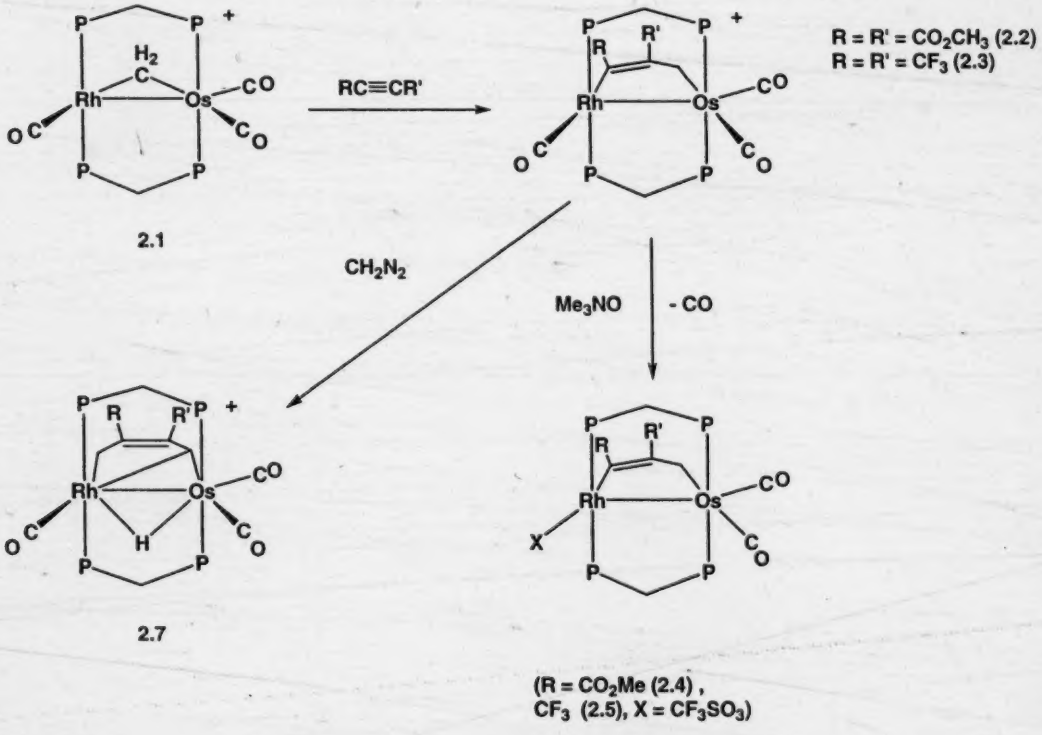

Scheme 2.1. *Generating C_3- and C_4-bridged species from compound **2.1**.*

Each of these new complexes has the expected $^{31}P\{^1H\}$ NMR pattern with one high-field signal corresponding to the Os-bound phosphines, and one low-field signal from the Rh-bound phosphines, displaying the typical coupling to this metal. In

compound **2.2**, for example, the Rh-bound phosphines, appearing as a doublet of multiplets at δ 26.6, display the anticipated coupling to Rh of 113 Hz whereas the Os-bound phosphines appear as a multiplet at δ -1.5. In the ^{1}H NMR spectrum, the two dppm methylene signals (δ 3.94 and 4.96) indicate that the molecule possesses 'front-back' asymmetry, whereas the metal-bound CH_2 signal appears at higher field (δ 1.68) as a triplet ($^{3}J_{PH}$= 3.1 Hz) showing coupling to only the osmium-bound phosphines, as determined by selective $^{1}H\{^{31}P\}$ NMR experiments. The absence of coupling of this methylene group to Rh or to the Rh-bound phosphines suggests that alkyne insertion into the Rh-CH_2 bond has occurred. Repeating the reaction using a sample of compound **2.1** that was ^{13}C enriched in the μ-CH_2 position yields a product that displays a high-field triplet at δ 7.7 (J_{PC}= 7 Hz), in the $^{13}C\{^{1}H\}$ NMR spectrum, and the absence of Rh coupling again indicates that this fragment is bound to the Os centre, confirming that alkyne insertion into the Rh-CH_2 bond has occurred. All carbonyls in the complex were identified as being terminal on the basis of the $^{13}C\{^{1}H\}$ NMR spectrum of ^{13}CO-labeled sample of compound **2.2**, with one CO on Rh at δ 191.3 with 51 Hz coupling to the metal, and two on Os at δ 183.7 and 171.4 displaying 11 and 12 Hz coupling, respectively, to the Os-bound phosphines.

The crystal structure of compound **2.2**[8] confirms that insertion of the alkyne into the Rh-CH_2 bond has taken place and a representation of the complex cation is shown in Figure 2.1. Selected bond lengths and angles are presented in Table 2.3. The dppm ligands are in a trans bridging geometry at both metals, as is typical for an A-frame complex. At Os, the geometry is octahedral with two sites occupied by the two trans dppm ligands. In addition, one carbonyl lies opposite the Rh-Os bond while the other is

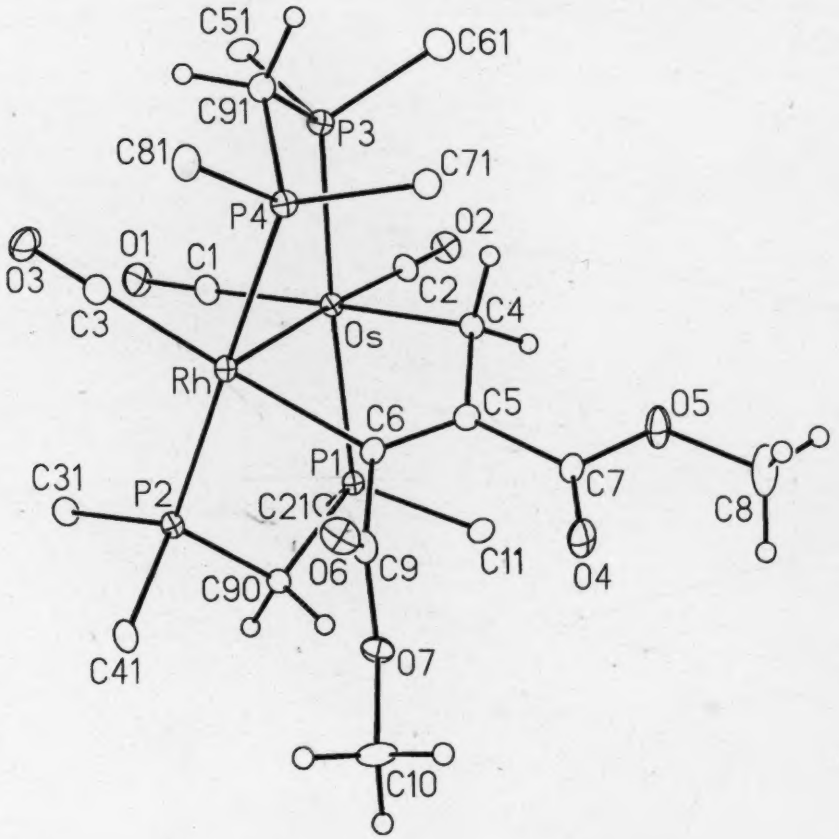

Figure 2.1 *Perspective view of the [RhOs(CO)3(μ–η1:η1–MeO2CC=C (CO2Me)CH2)-(dppm)2]+ complex cation of compound* **2.2** *showing the atom labelling scheme. Non-hydrogen atoms are represented by Gaussian ellipsoids at the 20% probability level. Only the ipso carbons of the phenyl rings are shown. Methylene and methyl hydrogens are shown with arbitrarily small thermal parameters.*

Table 2.3. Selected Distances (Å) and Angles (deg) for compound **2.2.**

Atom1	Atom2	Distance
Os	Rh	2.792(7)
Os	P(1)	2.397(2)
Os	P(3)	2.385(2)
Os	C(1)	1.949(9)
Os	C(2)	1.864(9)
Os	C(4)	2.180(8)
Rh	P(2)	2.323(2)
Rh	P(4)	2.345(2)
Rh	C(3)	1.907(1)
Rh	C(6)	2.067(9)
C(4)	C(5)	1.507(1)
C(5)	C(6)	1.325(1)
P1	P2	3.035(3)[§]
P3	P4	3.041(3)[§]
O(1)	C(1)	1.127(1)
O(2)	C(2)	1.114(1)
O(3)	C(3)	1.130(1)

[§] Non-bonded distance

Atom1	Atom2	Atom3	Angle
Rh	Os	P(1)	90.28(5)
Rh	Os	P(3)	90.85(6)
Rh	Os	C(1)	92.0(3)
Rh	Os	C(2)	174.6(3)
Rh	Os	C(4)	83.1(2)
P(1)	Os	P(3)	176.17(8)
C(1)	Os	C(2)	93.4(4)
C(1)	Os	C(4)	175.1(3)
C(2)	Os	C(4)	91.5(3)
Os	Rh	P(2)	90.15(6)
Os	Rh	P(4)	90.73(6)
Os	Rh	C(3)	93.9(3)
Os	Rh	C(6)	83.6(2)
P(2)	Rh	P(4)	178.65(8)
P(2)	Rh	C(3)	92.2(3)
C(3)	Rh	C(6)	177.2(4)
Os	C(4)	C(5)	113.9(6)
C(4)	C(5)	C(6)	122.4(8)
Rh	C(6)	C(5)	124.3(7)

trans to the methylene groups of the C_3-bridged fragment. At rhodium, the geometry is a square-based pyramid in which the four basal sites are occupied by the mutually trans phosphines and the carbonyl which is trans to one of the carbons from the inserted alkyne. A vacant coordination site on Rh lies opposite to the metal-metal bond. The molecule is significantly twisted about the metal-metal bond into a staggered conformation such that the torsion angles about the Rh-Os bond range from 25.4(3)° to 28.12(8)°. Within the C_3 fragment, the variation in C-C bond lengths is in agreement with the formulation shown in Scheme 2.1. Therefore, the C(6)-C(5) bond length (1.33(1) Å) is typical of a C=C double bond while C(4)-C(5) (1.51(1)Å) is typical of a single bond between sp^3 and sp^2 carbons.[9] The angles within the C_3 unit also reflect these hybridization schemes, in which the Rh-C(6)-C(5) and C(6)-C(5)-C(4) angles (124.3(7)°, 122.4(8)°) are typical of sp^2 carbons, while the Os-C(4)-C(5) angle (113.9(6)°) is close to the expected value for sp^3 hybridization. It is noteworthy, however, that all angles are somewhat larger than the idealized values, suggesting strain within the dimetallacyclopentene moiety. This strain is probably responsible for the staggered arrangement of the ligands in both metals, as noted above. An eclipsed conformation would require the angles within the metallacycle to open up even further from the idealized values creating substantial strain within this dimetallacycle. The difference in the Os-C(4) (2.180(8) Å) and Rh-C(6) (2.067(4) Å) distances probably also reflects the differences in hybridization of these carbons; the radius of an sp^2 carbon (0.74 Å) is less than that of an sp^3 carbon (0.77 Å)[10] although some additional shortening because of π back donation into a π^* orbital on the vinylic carbon is also possible. The metal-metal distance of 2.7915(7) Å is typical of a single bond between the metals, and is

significantly shorter that the intraligand P-P distances, both of which are approximately 3.04 Å, showing a substantial attraction of the metals. We view the metal-metal interaction as a dative bond resulting from donation of the pair of electrons in the Rh d_z^2 orbital into a vacant Os orbital giving the latter metal its favoured 18e configuration. In this bonding formulation, Rh is in the +1 oxidation state while Os is +2; both represent common oxidation states for these metals. The formulation in which a conventional metal-metal bond is involved would have Rh in a +2 oxidation state and Os as +1; neither are common oxidation states for these metals.

The HFB-insertion product, $[RhOs(CO)_3(\mu\text{-}\eta^1\text{:}\eta^1\text{-}(F_3C)C{=}C(CF_3)CH_2)\text{-}(dppm)_2]^+$ (**2.3**) is spectroscopically very similar to compound **2.2**. Again, the spectroscopy makes it clear that insertion of the HFB molecule into the$Rh\text{-}CH_2$ bond has occurred. Attempts to obtain X-ray quality crystals of compound **2.3** invariably met with failure except on one occasion when a few X-ray quality crystals were found among the bulk sample crystallized from CD_2Cl_2. However, determination of the structure has established that the crystal analyzed is comprised of disordered molecules of compound **2.3** and $[RhOsCl(CO)_2(\mu\text{-}\eta^1\text{:}\eta^1\text{-}(CF_3)C{=}C(CF_3)CH_2)(dppm)_2]$ (**2.6**), present in the crystal in equal amounts. Presumably, the latter product results from chloride abstraction from the solvent. Attempts to synthesize this product by rational routes such as carbonyl removal in the presence of chloride ions failed. The complex cation of compound **2.3** is not shown since the structure is quite similar to compound **2.2** (shown is Figure 2.1) and all atoms of compound **2.3** were found to be superimposed with that of compound **2.6**, which is shown in Figure 2.2. Bond lengths and angles of both compounds are presented in Table 2.4 (recall that both compounds are identical except for the disordered Cl and

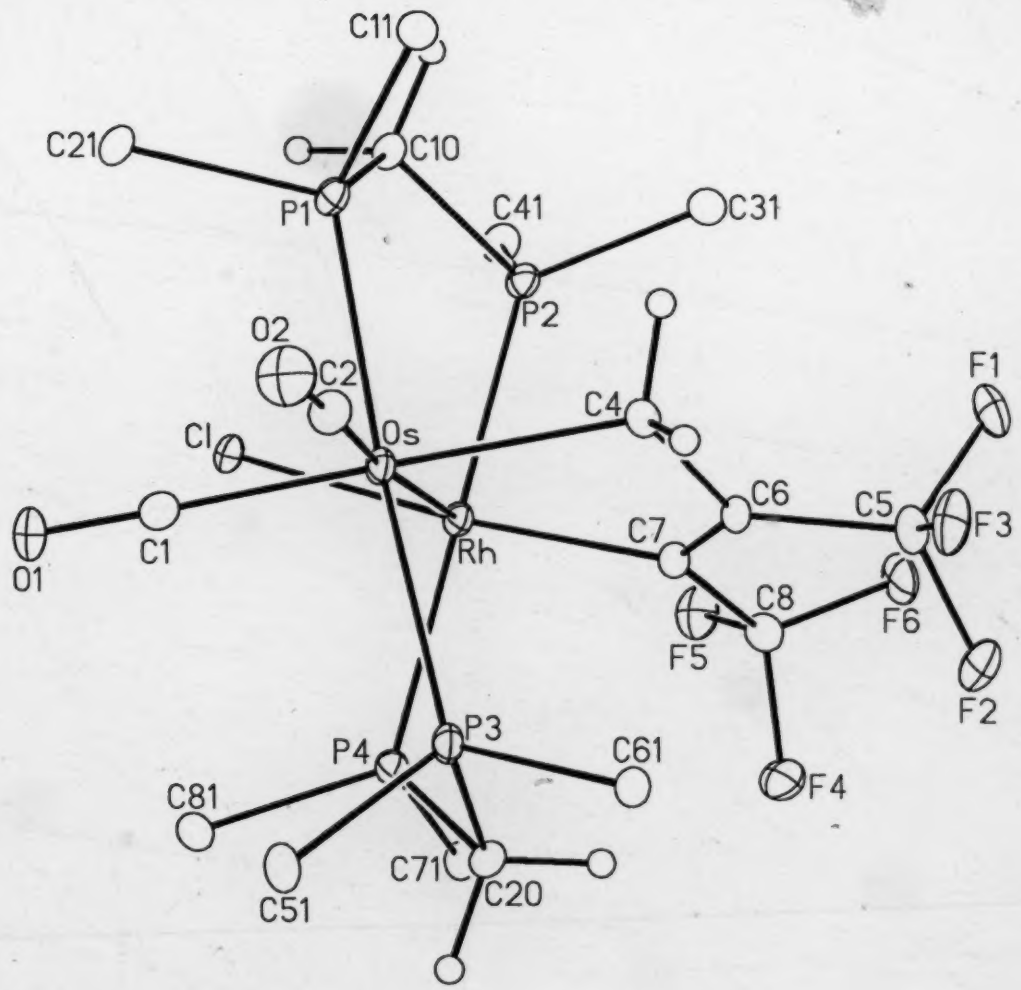

Figure 2.2. *Perspective view of the [RhOsCl(CO)$_2$(μ-η^1:η^1-(CF$_3$)C=C(CF$_3$)-CH$_2$)(dppm)$_2$]$^+$ (2.6) molecule showing the atom labelling scheme. Non-hydrogen atoms are represented by Gaussian ellipsoids at the 20% probability level. Hydrogen atoms are shown arbitrarily small and only the ipso carbons of the phenyl rings are shown for clarity.*

Table 2.4 Selected Distances (Å) and Angles (deg) for compounds **2.3** and **2.6.**

Atom1	Atom2	Distance	Atom1	Atom2	Atom3	Angle
Os	Rh	2.7582(6)	Rh	Os	P1	89.29(5)
Os	P(1)	2.381(2)	Rh	Os	P3	91.70(5)
Os	P(3)	2.394(2)	Rh	Os	C1	89.5(2)
Os	C(1)	1.928(8)	Rh	Os	C2	176.1(2)
Os	C(2)	1.870(8)	Rh	Os	C4	83.5 (2)
Os	C(4)	2.203(7)	P1	Os	P3	176.04(6)
Rh	Cl	2.418(7)	C1	Os	C4	173.0(3)
Rh	P(2)	2.319(2)	C2	Os	C4	93.3(3)
Rh	P(4)	2.319(2)	Os	Rh	Cl	99.1(1)
Rh	C(3)	1.90(2)	Os	Rh	P2	94.40(5)
Rh	C(7)	2.054(7)	Os	Rh	P4	88.05(5)
C(6)	C(7)	1.35(1)	Os	Rh	C3	94.8(7)
C(4)	C(6)	1.49(1)	Os	Rh	C7	85.2(2)
P(1)	P(2)	3.073(3)[b]	Cl	Rh	C7	173.2(2)
P(3)	P(4)	2.992(3)[b]	P2	Rh	P4	177.46(7)
O(1)	C(1)	1.143(9)	C3	Rh	C7	173.6(7)
O(2)	C(2)	1.147(9)	Os	C4	C6	113.4(5)
O(3)	C(3)	1.01(3)	C4	C6	C7	122.3(6)

[a] Compounds **2.3** and **2.6** are superimposed in the X-ray structure determination. The parameters involving C(3)O(3) refer to compound **2.3** while those involving Cl refer to compound **2.6**. See the Experimental section for a description of the disorder.

[b] Non-bonded distance

C(3)O(3) ligands and the presence of the triflate anion in the former). The structures of compounds **2.3** and **2.6** are very similar to that of **2.2**, confirming that insertion of the HFB molecule into the Rh-CH_2 bond has occurred, yielding the C_3-bridged "$(CF_3)C=C(CF_3)CH_2$" moiety. Both metals in compounds **2.3** and **2.6** have geometries very similar to that of **2.2** and again the structures are staggered along the Rh-Os bond with an average torsion angle of approximately 25.8° (22.7(3)-28.95(7)°). All parameters for compounds **2.3** and **2.6** agree to within 3 standard deviations with those of **2.2**. so again, the C(6) and C(7) distance (1.35 (1) Å), of the original alkyne group, is consistent with a double bond while the link between this and the methylene group (C(6)-C(4)), at 1.49 (1) Å is consistent with a single bond. All angles within the dimetallacycle are also in good agreement and again suggest strain that results in skewing of the structure about the metal-metal bond.

Removal of a carbonyl from compounds **2.2** and **2.3** by the reaction with trimethylamine N-oxide results in the formation of two new species, $[RhOs(CF_3SO_3)(CO)_2(\mu,\eta^1:\eta^1\text{-}(CO_2CH_3)C=C(CO_2CH_3)CH_2)(dppm)_2]$ (**2.4**) and $[RhOs(CF_3SO_3)(CO)_2(\mu,\eta^1:\eta^1\text{-}(CF_3)C=C(CF_3)CH_2)(dppm)_2]$ (**2.5**) as diagrammed in Scheme 2.1. The $^{31}P\{^1H\}$ NMR spectrum of each compound suggests that they are fluxional at room temperature, as the signals for both sets of phosphines are broad. Cooling the solutions to –80°C shows the low temperature limiting spectra of these species, which appear as ABCDX patterns in the $^{31}P\{^1H\}$ NMR spectra in which the Rh-bound phosphines appear as overlapping multiplets between δ 26 and 29, while the Os-bound phosphines appear between δ –4 and –5. This pattern was unexpected, as characterization of compound **2.4** led us to believe that it was isostructural to both **2.2** and **2.3**, and therefore would display

a similar $^{31}P\{^1H\}$ NMR spectrum. However, twisting of the molecule about the Rh-Os, as shown in Figures 2.1 and 2.2 renders all four phosphorus chemically inequivalent. Rapid oscillation about this metal-metal bond averages the pairs of ^{31}P nuclei on each metal to give an AA'BB'X spin system, while in the static structure all four phosphorus nuclei are inequivalent. The bulky triflate may inhibit oscillation about the metal-metal bond, allowing observation of the static structure. The osmium-bound methylene signal in **2.4** remains a triplet at δ 1.06 ($^1J_{CH}$= 130 Hz) in the ^1H NMR spectrum, still only displaying coupling to the Os-bound phosphines. The two remaining carbonyl ligands appear in the $^{13}C\{^1H\}$ NMR spectrum at δ 188.3 and 174.6, indicating they are terminally bound groups, as have been confirmed in the IR with stretches at 2012 and 1908 cm^{-1}. The absence of a coupling of either carbonyl to Rh, suggests that they are bound to Os, leaving Rh electron deficient. In order to alleviate this electron deficiency at rhodium, we believe that the metal may have coordinated the anion. Unfortunately, the IR data cannot unambiguously confirm the presence of triflate ion coordination, due to the presence of several stretches in the region where both coordinated and uncoordinated triflate would be observed. In order to confirm anion coordination, an $^{19}F\{^1H\}$ NMR spectrum, using the BF_4^- salt would be useful.

It was anticipated the removal of one of the carbonyls from **2.2** might induce a switch in the binding mode of the ligand as shown in Figure 2.3. Conversion of the C_3 ligand in **G** from a 2-electron donor to a 4-electron donor in **H** would alleviate the electron deficiency brought about by ligand loss. If the transformation had taken place, the μ-CH_2 group from compound **2.1** should change hybridization from sp^3 to sp^2, which

Figure 2.3. *Two configurations of C_3-bridged complexes.*

would in turn raise the C-H coupling constant. However, from labelling studies, the C-H coupling constant obtained was 128 Hz, a value that is typical for sp^3 hybridization and in good agreement with that observed in **2.2**, which has the C_3 bridge.we propose for **2.4**. The structure proposed for **2.4** is also analogous to that established for **2.6** in X-ray structure determinations, with a triflate ion replacing chloride.

Although compound **2.3** does not react further with diazomethane, compound **2.2** does react to yield the C_4-bridged product, $[RhOs(CO)_3(\mu\text{-}\eta^1\text{:}\ \eta^1\text{-}CH_2(CH_3O_2C)C\text{=}C(CO_2CH_3)CH)(\mu\text{-}H)(dppm)_2][CF_3SO_3]$ (**2.7**), shown in Scheme 2.1. The ^1H NMR spectrum of **2.7** displays the typical dppm methylene signals at δ 5.14 and 4.32. Also observed in the ^1H NMR spectrum is an additional methylene signal at δ 4.07 showing coupling of 2.2 Hz to Rh and 11 Hz to the Rh-bound phosphines, a single hydrogen at δ 5.29, displaying 2 Hz coupling to Rh and 4 Hz coupling to the Os-bound ^{31}P nuclei, and a hydride signal at δ -16.5. The 12 Hz coupling of this hydride signal to Rh and its coupling to all four phosphorus nuclei indicate that it bridges the metals. When a $^{13}CH_2$-enriched sample of **2.2** (**2.2**-$^{13}CH_2$) is used (generated from $^{13}CH_2$-enriched **2.1**), the single hydrogen at δ 5.29 displays 161 Hz coupling to the ^{13}C nucleus. The $^{13}C\{^1H\}$ NMR signal from this μ-CH group appears at δ 118.3 with 16 Hz coupling to Rh, and the signal for the new CH_2 group is found at δ 70.3 with a 25 Hz coupling to Rh. The

structure proposed in Scheme 2.1 is consistent with the spectral data, in which the added methylene group is clearly bound to Rh, while the original CH_2 group of compound **2.2** has undergone C-H activation to yield the methyne-bridged group and the bridging hydride. The chemical shift for this carbyne carbon and the C-H coupling constant (^1J= 161 Hz) are consistent with previous determinations.[11a]

The C_2-bridged species, $[RhOs(CO)_3(\mu\text{-}\eta^1\text{:}\eta^1\text{-}(R)C{=}C(R))(dppm)_2][CF_3SO_3]$ (R= CO_2Me (**2.8**), CF_3 (**2.9**)), have been previously reported,[4] and we now find that both species react with diazomethane, although they yield very different products. In the reaction with CH_2N_2, compound **2.8** yields three different products depending upon the reaction temperature. At –80°C, the reaction with diazomethane yields exclusively the product $[RhOs(CO)_3(\mu\text{-}\eta^1\text{:}\eta^1\text{-}CH_2(R)C{=}C(R))(dppm)_2][CF_3SO_3]$ (R= CO_2Me, (**2.10**)), in which methylene insertion into the Rh-alkyne bond has occurred. In addition to the dppm methylene groups, the diazomethane-generated methylene group appears as a multiplet at δ 4.82 in the ^1H NMR. If $^{13}CH_2N_2$ is used in the reaction the methylene carbon appears at δ 100.5, and displays 28 Hz coupling to Rh, confirming that it has inserted into the Rh-C bond, and in the same sample the methylene hydrogens of this group display a 152 Hz coupling to the carbon. Again, from the two distinct ^1H NMR shifts of the dppm groups, it is seen that the molecule does not possess front-back symmetry. Three terminally bound carbonyls are present at δ 200.4 ($^1J_{RhC}$= 49 Hz, $^2J_{PC}$= 14 Hz), 192.9, and 176.6 ($^2J_{PC}$= 9 Hz) consistent with the structure shown in Scheme 2.2, in which one is bound to Rh, and two to Os.

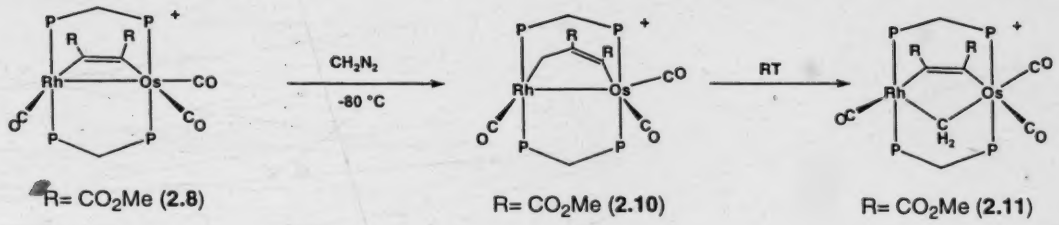

Scheme 2.2. *Reactivity of C_2 alkyne-bridged compounds with diazomethane.*

If the reaction of **2.8** with an excess of diazomethane is carried out at low temperatures and allowed to warm, compound **2.11** forms (See Scheme 2.2). Its $^{31}P\{^1H\}$ NMR spectrum has a doublet of multiplets at δ 32.3 and another multiplet at δ 0.6 from the Rh- and Os-bound phosphines, respectively. In this species, as with **2.10**, there has been only one CH_2 unit added, however now it is in a position bridging the metals. Whether the transformation from compound **2.10** to compound **2.11** is a result of the initial insertion followed by rearrangement, or if it is simply a different "CH_2" group that has been added to the framework has not yet been determined. It is our speculation that complex **2.11** forms as a result of loss of the original methylene group and an additional methylene unit taking on the bridging position. Three methylene signals appear in the ^1H NMR spectrum of compound **2.11**. Two methylene signals are from the dppm groups, which are found to resonate at δ 4.01 and 3.89, while the diazomethane-generated CH_2 group appears at δ 1.32 ($^1J_{CH}$= 128 Hz) and shows coupling to both sets of phosphines, suggesting that it bridges the two metals. From the addition of ^{13}C-Diazald to compound **2.8**, the bridging methylene carbon was observed at δ 30.6 in the $^{13}C\{^1H\}$ NMR spectrum, and was found to have 33 Hz coupling with Rh, and 13 Hz coupling to all four ^{31}P nuclei. The carbonyl carbons appear as a doublet of triplets at δ 190.8 ($^1J_{RhC}$= 52Hz,

$^2J_{PC}$= 12Hz) and two multiplets at δ 190.7 and δ 169.6. We have previously reported the formation of similar compounds both in a dirhodium compound[11b] and a Rh/Ru compound.[11a] In the Rh/Ru analogue of compound **2.11**, in which one CO has been replaced by a coordinating triflate anion prior to exposure to diazomethane, the product of insertion into the Rh-alkyne bond was not observed. Whether such a species was formed, but had too short a lifetime to allow its observation or whether reaction with diazomethane proceeded directly to the methylene-bridged product , analogous to **2.11**, is not known.

When compound **2.9** is reacted with diazomethane, only $[RhOs(CO)_4(\mu\text{-}CH_2)(dppm)_2][CF_3SO_3]$ (**1.2**) and $[RhOs(CO)_3(\mu\text{-}\eta^1\text{:}\eta^1\text{-}(F_3C)C{=}C(CF_3)CH_2)(dppm)_2]^+$ (**2.3**) are observed in a 1:1 ratio as the major products along with minor amounts of unidentified products in the $^{31}P\{^1H\}$ NMR spectrum. This was somewhat surprising given the chemistry reported above for the DMAD analogue and a previous report in which methylene insertion into the Rh-Rh bond of an HFB-bridged species gave a product very similar to that of **2.11**.[11b]

Discussion

The heterobinuclear complex $[RhOs(CO)_4(dppm)_2][X]$ (**1.1**) has been found to add four methylene groups to ultimately yield either $[RhOs(CO)_3(C_4H_8)(dppm)_2][X]$ (**1.3**) or $[RhOs(CH_3)(\eta^1\text{-}C_3H_5)(CO)_3(dppm)_2][X]$ (**1.4**).[1b] This has been shown to proceed through the sequential addition of methylene groups between the metals. After addition of the first methylene group, subsequent additions occur into the Rh-CH_2 bond of the bridging hydrocarbyl fragments of the intermediate species (see Scheme 1.6). The

pivotal species that yields either the butanediyl or allyl methyl compounds in this chemistry is proposed to be a propanediyl (C_3H_6)-bridged intermediate. In this study, we set out to model this C_3H_6-bridged species by combination of methylene groups as C_1 fragments and alkynes as C_2 fragments. In principle, a C_3-bridged species can be obtained by the reaction of a methylene-bridged precursor with an alkyne or by the reaction of an alkyne-bridged precursor with diazomethane. As outlined in Scheme 2.3, if substrate coordination and subsequent insertion occurs at Rh, these different strategies should result in different isomers having the methylene unit either adjacent to Os or to Rh. In both cases, insertion occurs into the rhodium-carbon bond, presumably due to the coordinative unsaturation at the Rh centre.

Although alkynes do not react with the methylene-bridged tetracarbonyl $[RhOs(CO)_4(\mu\text{-}CH_2)(dppm)_2][CF_3SO_3]$ (**1.1**), reaction occurs readily with the tricarbonyl species $[RhOs(CO)_3(\mu\text{-}CH_2)(dppm)_2][CF_3SO_3]$ (**2.1**).[3] In the case of both DMAD and HFB, facile insertion of the alkynes into the Rh-CH_2 bond occurs, yielding $[RhOs(CO)_3(\mu\text{-}\eta^1\text{:}\eta^1\text{-}RC{=}CRCH_2)(dppm)_2][CF_3SO_3]$ (R=R'= CO_2Me (**2.2**), CF_3 (**2.3**)). Spectroscopic investigations and the X-ray crystal structure determinations establish the bridged η^1:η^1 coordination mode for these C_3 units much as had been proposed for the C_3H_6-bridged intermediate in the above methylene-coupling sequence. This geometry also models products of the coupling of methylene groups and olefins as reported by

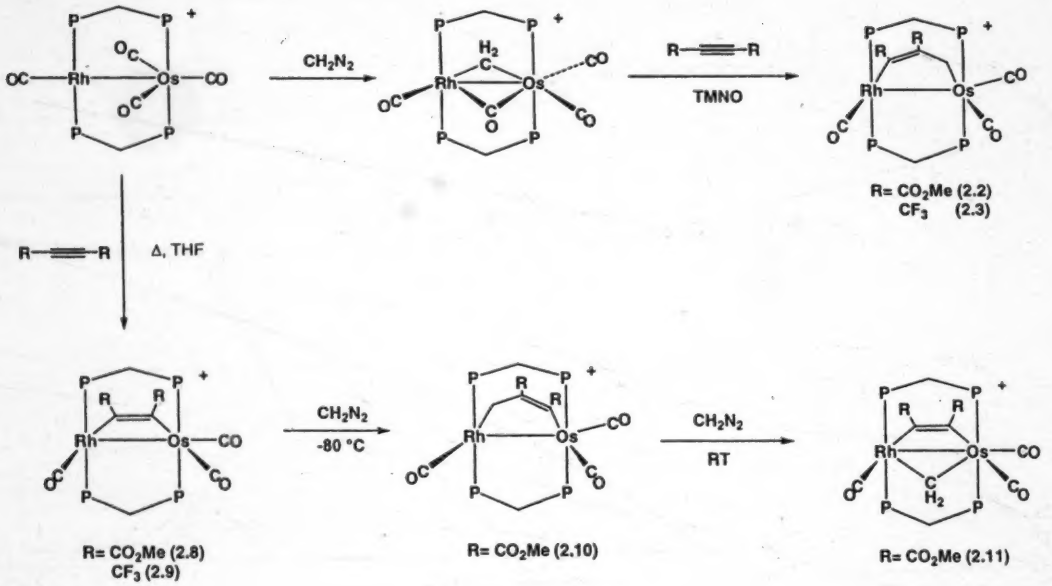

Scheme 2.3. *A comparison of two synthetic routes to isomeric C_3 products.*

Dry,[2] in his proposal for **FT** chain growth, and by Pettit and others[12] for reactions of ethylene with "M(μ-CH_2)M" units in homogeneous complexes. Presumably, one reason for the stability of our "C_3-bridged" product and the instability of those resulting either from methylene coupling or from methylene and olefin coupling is the absence of β-hydrogens in our product and their presence in the latter cases. β-Hydrogen elimination is presumably the reason behind the transformation of the putative propanediyl-bridged species in the Dry scheme into a surface-bound propene group.

Similar combinations of alkynes and a methylene fragment were observed in the related RhRu[11a] complex [RhRu(CO)$_3$(μ-CH)$_2$(dppm)$_2$][CF_3SO_3] to give a series of products, [RhRu(CO)$_3$(μ-η^1:η^1-(R)C=C(R)CH_2)(dppm)$_2$][CF_3SO_3], analogous to **2.2** and **2.3**. Although there are other reports of alkyne insertions into "M(μ-CH_2)M" groups,[13] the work in our group on alkyne insertion into "Rh(μ-CH_2)M" (M= Ru, Os) is the first to

yield the "M(μ-η^1:η^1-(R)C=C(R)CH_2)M" fragment (structure **G** in Figure 2.3), while other related work yielded the bridging vinyl carbene groups (**H**). A comparison of the two ligand types was shown earlier in Figure 2.3. Essentially, the ligand connectivity is the same in both cases, and they differ only in their binding to the metals. In **G** the ligand functions as a 2-electron donor, while in **H** it functions as a 4-electron donor. This led us to suggest that conversion of binding mode **G** into **H** might be induced in our system through the loss of a carbonyl ligand. The assumption was that the loss of the 2-electron donor carbonyl ligand might be compensated for by a change in the ligand binding mode from **G** to **H**. However, attempts to promote this transformation by the removal of a carbonyl from **2.3** by TMNO did not result in the targeted ligand rearrangement, but instead resulted in the coordination of the triflate or tetrafluroroborate anion at Rh to give [RhOs(X)$(CO)_2$(μ-η^1:η^1-RC=CR'CH_2)$(dppm)_2$] (X= $CF_3SO_3^-$, R=R'= CO_2Me (**2.4**), CF_3 (**2.5**)). In this case, the anion supplies the pair of electrons lost by the ejection of a carbonyl. It is assumed that the structures of the triflate adducts are analogous to that of the chloride, determined in this study. It would be of interest to establish whether the above targeted ligand rearrangement (Figure 2.3) could be induced if the coordinating triflate or tetrafluoroborate anions were replaced by bulky, non-coordinating anions such as tetraphenylborate. This was not attempted.

The above observation is an interesting contrast to the analogous reaction for the RhRu analogue.[11a] As shown in Scheme 2.4, carbonyl loss from [RhRu$(CO)_3$(μ-η^1:η^1-(R)C=C(R)CH_2)$(dppm)_2$][CF_3SO_3] did *not* result in triflate or tetrafluoroborate coordination as observed herein, but instead gave an interesting transformation wherein a 1,3-hydrogen shift yielded an isomer of the targeted vinyl carbene species. We assume

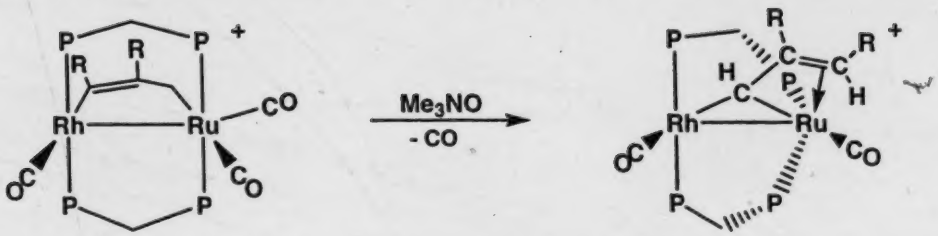

I J

Scheme 2.4. *Reactivity of a Rh/Ru complex with DMAD.*

that the targeted vinyl carbene product was the initial product in this transformation, but that subsequent rearrangement occurred to yield the product **J** in Scheme 2.4. It is not clear why this dramatic reactivity difference results from replacement of Os by Ru, however, we speculate that the stronger Os-CH_2 *versus* Ru-CH_2 bonds[14] in the precursors favours retention of the original bridged structure and the strong Os-CH_2 bond does not allow the necessary rearrangement to the vinyl carbene species.

Since compounds **2.2** and **2.3** were synthesized as models for C_3 intermediates it was of interest to determine if it was possible to transform them into C_4 products. Attempts to add a C_1 fragment in the form of a methylene group from diazomethane failed with compound **2.3**, which did not react. However, the reaction of compound **2.2** with diazomethane yielded the C_4-bridged product, $[RhOs(CO)_3(\mu\text{-}\eta^1\text{:}\eta^2\text{-}CH_2(MeO_2C)\text{-}C{=}C(CO_2Me)CH)(\mu\text{-}H)(dppm)_2][X]$ (**2.7**). It appears that compound **2.2** is a reasonable model for the propanediyl-bridged intermediate **C** (see Scheme 1.6), having an analogous bridged $\eta^1\text{:}\eta^1$ coordination mode and incorporating an additional CH_2 group to give a C_4-bridged product. However, there are some notable differences as summarized in Scheme 2.5 (other ligands have been omitted for clarity). First, addition of a methylene group to

2.2 resulted in C-H activation and a metal hydride product (**N**), and second, the resulting C_4 unit remains bridging the metals, unlike the butanediyl product **1.3**, in which the hydrocarbyl fragment ends up chelating on Os. The formation of a metal hydride through C-H activation was initially not a complete surprise. In the butanediyl product **1.3** (species **L** in Scheme 2.5), one of the methylene groups was found to be involved in an agostic interaction with Rh. It is assumed that this agostic interaction observed previously had, in our chemistry, resulted in C-H activation. However, labelling studies have established that although in compound **1.3** it is the last-added CH_2 group that forms the agostic interaction, in compound **2.7**, it is the *initial* CH_2 group for which C-H activation occurs, not the *added* CH_2 group. In both cases the initial product of CH_2 insertion into the Rh-C bond is likely the C_4-bridged species **K** and **M**, shown in Scheme

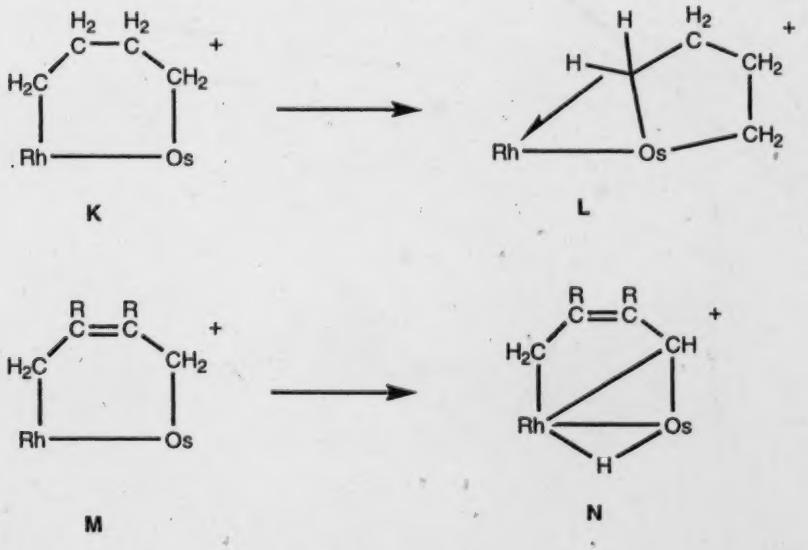

Scheme 2.5. *A comparison of two C_4 products obtained through diazomethane addition.*

2.5. Intermediate **K** can clearly give the osmacyclopentane product **L** by migration of the Rh-bound CH_2 group to Os, while the unsaturated intermediate, **M**, gives the C-H activation product **N**. It is not clear what subtle differences in electronic structure or ring strain within the two intermediates, **K** and **M**, or in the products, gives rise to this difference in reactivity.

An explanation is not evident for the failure of compound $[RhOs(CO)_3(\mu\text{-}\eta^1\text{:}\eta^1\text{-}(F_3C)C{=}C(CF_3)CH_2)(dppm)_2]^+$ (**2.3**) to react with diazomethane (especially when the analogous DMAD product does), and for the inability of the Rh/Ru analogues of **2.2** and **2.3** to react with diazomethane.[9a] Clearly, subtle electronic differences in these complexes can give rise to dramatic differences in reactivity.

As noted in the introduction, it was anticipated that generation of C_3-bridged products could result from reaction of a methylene-bridged precursor with alkynes, or from alkyne-bridged precursors with diazomethane. The above discussion indicates that the former route succeeded, and we have also partially succeeded by the second route. The reaction of $[RhOs(CO)_3(\mu\text{-}(CF_3)C{=}C(CF_3))(dppm)_2][CF_3SO_3]$ (**2.9**) with diazomethane does not yield the targeted product and instead yields a 1:1 ratio of $[RhOs(CO)_4(\mu\text{-}CH_2)(dppm)_2][CF_3SO_3]$ (**1.2**) and compound **2.3** determined through NMR. Although formation of the second product initially suggested that insertion of the methylene group into the Os-C bond had occurred, this seemed unlikely in view of *all* previous studies[1a,b,3,11a] that indicated exclusive insertion into the Rh-C bond. Maintaining this reaction at -80°C and monitoring the reaction by $^{19}F\{^1H\}$ NMR spectroscopy, shows the presence of free hexafluoro-2-butyne in solution, indicating that alkyne dissociation occurs at some stage in the reaction. Apparently, product **2.3** occurs

by alkyne insertion into the Rh-CH_2 bond of compound **2.1**, generated upon alkyne loss. The formation of the tetracarbonyl **1.2** from a tricarbonyl precursor is somewhat problematic, but we assume that CO is scavenged by **2.1** from a variety of decomposition products, some of which can be seen in the $^{31}P\{^1H\}$ NMR spectrum of the reaction mixture.

The reaction of **2.8** with diazomethane proceeds quite differently, yielding initially at -80°C, $[RhOs(CO)_3(\mu\text{-}\eta^1\text{:}\eta^1\text{-}CH_2(CO_2Me)C{=}C(CO_2Me))(dppm)_2][CF_3SO_3]$ (**2.10**), the targeted product of methylene insertion into the Rh-C bond. As noted earlier, this is an isomer of **2.2**, with the methylene bound to Rh instead of to Os. Like its isomer, compound **2.10** reacts further with diazomethane at ambient temperature. However, a C_4-bridged product is not obtained in this case. Instead another isomer, $[RhOs(CO)_3(\mu\text{-}CH_2)(\mu\text{-}\eta^1\text{:}\eta^1\text{-}(CO_2Me)C{=}C(CO_2Me))(dppm)_2][CF_3SO_3]$ (**2.11**) is obtained in which the methylene group is now bridging the metals, opposite the alkyne bridge. Further studies are underway to determine how the transformation of **2.10** to **2.11** occurs. One possibility is a second CH_2 insertion into the Rh-CH_2 bond in **2.10** occurs, but that ethylene extrusion occurs to regenerate **2.8**, and that at higher temperatures, insertion into the metal-metal bond of **2.8** is favoured over insertion into the Rh-alkyne bond. Further reaction of **2.11** with diazomethane occurs at ambient temperature to give a still unidentified product. When labelled $^{13}CH_2N_2$ is added to compound **2.8**, initial characterization of this product reveals four doublets in the $^{13}C\{^1H\}$ NMR spectrum, each with roughly 33 Hz carbon-carbon coupling. Selective $^{13}C\{^{31}P\}$ NMR experiments showed no change in the spectrum when either set of phosphines were decoupled, and thus we could not identify the metal to which these carbons were attached. No significant

Rh coupling was observed in any of the carbon signals. From mass spectrometry, the parent ion and isotope pattern matches that for a compound that has added four methylene units to the framework of compound **2.8**. Again, further work is ongoing to establish the nature of this species.

Reaction of the Rh/Ru analogue[11], $[RhRu(CF_3SO_3)(CO)_2(\mu\text{-}(CO_2Me)C{=}C\text{-}(CO_2Me))(dppm)_2]^+$ with diazomethane does not give a product of insertion into the Rh-alkyne bond and instead proceeds to only the alkyne- and methylene-bridged product, $[RhRu(CF_3SO_3)(CO)_2(\mu\text{-}(CO_2Me)C{=}C(CO_2Me))(dppm)_2]^+$, analogous to product **2.11**. There are two possibilities in this Rh/Ru system that we were unable to differentiate. Either initial insertion into the Rh-alkyne bond occurs, and that product rapidly proceeds to the product in which the methylene group bridges the metals, or the subtle differences in the metal combinations favours methylene insertion into the Rh-Ru bond rather than into the Rh-alkyne bond, never forming the initial insertion product seen in the Rh/Os chemistry. Again, a comparison of the RhOs chemistry reported herein with that of the analogous RhRu system shows that slight differences in the metal combination of each system can result in significant changes in reactivity and product formation.

Conclusions

We have demonstrated that our strategy to synthesize C_3-bridged fragments that are η^1 bound to each metal by combining alkynes as C_2 fragments and methylene groups as C_1 fragments has been successful. Two approaches gave initially isomeric products. Alkyne insertion into the Rh-CH_2 bond of a "Rh(μ-CH_2)Os' moiety gave species in which the Os-CH_2 bond was retained, whereas methylene insertion into the Rh-alkyne

bond of an alkyne-bridged "Rh(μ-RC=CR)Os" moiety retained the Os-alkyne bond. The metal combination seems important in two ways in these related transformations. First, the coordinative unsaturation of Rh results in substrate coordination at this metal with subsequent insertion into the Rh-C bond involving the bridging ligand. Second, the strength of the Os-C bond in the product also serves an important role. This is clearly seen in the stabilities of the isomers $[RhOs(CO)_3(\mu\text{-}\eta^1\text{:}\eta^1\text{-}(R)C{=}C(R)CH_2)(dppm)_2]^+$ and $[RhOs(CO)_3(\mu\text{-}\eta^1\text{:}\eta^1\text{-}CH_2(R)C{=}C(R))(dppm)_2]^+$. Only the product having the CH_2 group bound to Os is stable. That having the Rh-bound CH_2 group seems prone to extrusion of the CH_2 (possibly via ethylene loss after coupling of two CH_2 groups). Further reaction of the first isomer (**2.2**) with diazomethane to yield the C_4-bridged product strengthens our contention that our C_3-bridged products function as reasonable models for C_3 intermediates in C-C bond formation in **FT** chemistry. However, as with the methylene coupling previously reported, we failed to achieve higher that a C_4 fragment. It is also frustrating that the subtle differences between the unsaturated C_3- and C_4-bridged products reported in this chapter and the saturated analogues previously reported remain unexplained and are not understood. Additional studies should help unravel some of these problems.

References and Notes

1. (a) Rowsell, B.D.; Trepanier, S.J.; Lam, R.; McDonald, R.; Cowie, M. *Organometallics*, **2002**, *21*, 3228. (b) Trepanier, S. J.; Sterenberg, B. T.; McDonald, R.; Cowie, M. *J. Am. Chem. Soc.* **1999**, *121*, 2613. (c) Dell'Anna, M. M.; Trepanier, S. J.; McDonald, R.; Cowie, M. *Organometallics* **2001**, *20*, 88.

2. Dry, M. E. *Appl. Catal. A* **1996**, *138*, 319.

3. Trepanier, S.J.; Dennett, N.L.; Sterenberg, B.T.; McDonald, R; Cowie, M. *Manuscript to be Submitted.*

4. Hilts, R.W.; Franchuk, R.A.; Cowie, M. *Organometallics*. **1991**, *10*, 304.

5. Programs for diffractometer operation, data reduction, and absorption correction were those supplied by Bruker.

6. Sheldrick, G. M. *Acta Crystallogr. Sect. A* **1990**, *46*, 467.

7. Sheldrick, G. M. *SHELXL-93*: Program for crystal structure determination; University of Gottingen: Gottingen, Germany, **1993**,13.

8. Graham, T.W.; Cowie, M. *Unpublished results*.

9. Allen, F.H.; Kennard, O.; Watson, D.G.; Brammer, L.; Orpen, A.G.; Taylor, R. *J. Chem. Soc. Perkin Trans. II*, **1987**, S1.

10. Huheey, J.E.; Keiter, E.A.; Keiter, R.L. *Inorganic Chemistry– Principles of Structure and Reactivity 4th Ed.* p.292, HarperCollins College Publishers: New York, **1993**.

11. (a) Rowsell, B.D.; McDonald, R.; Cowie, M. *Organometallics*, **2003**, *22*, 2944. (b) McKeer, I. R.; Sherlock, S. J.; Cowie, M. *J. Organomet. Chem.* **1988**, *352*, 205.

12. (a) Sumner, C.E., Jr.; Riley, P.E.; Davis, R.E.; Pettit, R. *J. Am. Chem. Soc.* **1980**. *102*, 1752. (b) Sumner, C.E., Jr.; Collier, J.A.; Pettit, R. *Organometallics* **1982**, *1*, 1350.

13. (a) Dyke, A.F.; Knox, S.A.R.; Naish, P.J.; Taylor, G.E. *J. Chem. Soc. Chem. Commun.* **1980**, 803. (b) Gracey, B. P.; Knox, S. A. R.; Macpherson, K. A.; Orpen, A. G.; Stobart, S. R. *J. Chem. Soc. Dalton Trans.* **1985**, 1935. (c) Akita, M.; Hua, R.; Nakanishi, S.; Tanaka, M.; Morooka, Y. *Organometallics* **1997**, *16*, 5572, 37. (d)

Adams, P. Q.; Davies, D. L.; Dyke, A. F.; Knox, S. A. R.; Mead, K. A.; Woodward, P. *J. Chem. Soc. Chem. Commun.* **1983**, 222. (e) Colborn, R. E.; Dyke, A. F.; Knox, S. A. R.; Macpherson, K. A.; Orpen, A. G. *J. Organomet. Chem.* **1982**, *239*, C15. (f) Colborn, R. E.; Davies, D. L.; Dyke, A. F.; Knox, S. A. R.; Mead, K. A.; Orpen, A. G.; Guerchais, J. E.; Roue, J. *J. Chem. Soc.-Dalton Trans.* **1989**, 1799. (g) Kaneko, Y.; Suzuki, T.; Isobe, K.; Maitlis, P. M. *J. Organomet. Chem.* **1998**, *554*, 155.

14. Ziegler, T.; Tschinke, V.; Urenbach, B. *J. Am. Chem. Soc.* **1987**, *1*, 4825.

Chapter 3.

The Coupling of Cumulenes and Methylene Groups.

Introduction

As noted in Chapters 1 and 2, we are interested in modelling the stepwise coupling of methylene groups at a bimetallic core through the use of selected C_2 substrates and their coupling with methylene groups. In Chapter 2, we described the use of alkynes as the C_2 fragments and demonstrated that C_2-, C_3-, and C_4- bridged products could be sequentially accessed by the reaction of alkynes with diazomethane-generated CH_2 groups.

In this chapter, a similar strategy is described through the use of a series of cumulenes as the unsaturated substrates. Electronically and sterically, cumulenes such as allene ($H_2C=C=CH_2$) bear a greater resemblance to ethylene than do alkynes, so it was thought that this substrate, and some substituted derivatives, could function as better models than the products of alkyne insertion. The failure of ethylene to insert into the metal-carbon bond,[1] and the success of alkyne-insertion (Chapter 2) led us to believe that perhaps the additional π-system as well as the lack of β-hydrogens of the cumulenes would make them ideal substrates. Although allene and its substituted analogues are actually C_3 compounds, it is anticipated that upon reacting as shown in Scheme 1.8, only two of the carbons ultimately will insert into the Rh-CH_2 bond so it can be considered as functioning like a C_2 species. This chemistry is described herein.

Experimental

General Comments. All solvents were dried using the appropriate desiccants, distilled before use and stored under argon. Reactions were carried out under an argon atmosphere using standard Schlenk techniques. Allene gas was purchased from Praxair, while methylallene and dimethylallene were purchased from Fluka Chemicals. The trimethylphosphine was purchased from Aldrich as a 1.0 M solution in toluene. The ^{13}CO (99% enrichment) was purchased from Isotech, Inc. The complexes $[RhOs(CO)_4(\mu\text{-}CH_2)(dppm)_2][CF_3SO_3]$ (**1.2**),[2] and $[RhOs(CO)_3(\mu\text{-}CH_2)(dppm)_2][CF_3SO_3]$ (**2.1**)[3] were prepared as previously reported.

The ^1H, $^{13}C\{^1H\}$, ^1H-^1H COSY, and $^{31}P\{^1H\}$ NMR spectra were recorded on a Varian iNova-400 spectrometer operating at 399.8 MHz for ^1H, 161.8 MHz for ^{31}P and 100.6 MHz for $^{13}C\{^1H\}$. Infrared spectra were obtained on a Nicolet Magna 750 FTIR spectrometer with a NIC-Plan IR microscope either in the solid state or as a solution. The elemental analyses were performed by the microanalytical service within the department. Electrospray ionization mass spectra were run on a Micromass ZabSpec spectrometer by the staff in the mass spectrometry service laboratory. In all cases, the distribution of isotope peaks for the appropriate parent ion matched with that calculated for the formula given.

Preparation of Compounds

a) **$[RhOs(CO)_2(\mu\text{-}\eta^3\text{:}\eta^1\text{-}C(CH_2)_3)(dppm)_2][BF_4]$ (3.1).** 50 mg of $[RhOs(CO)_4(\mu\text{-}CH_2)(dppm)_2][BF_4]$ (**1.2**) (0.039 mmol) was dissolved in 15 mL of CH_2Cl_2. Allene was passed through this solution at a rate of 2 mL/min for two minutes. At this stage, no

Table 3.1. Spectroscopic Data For Compounds.

Compound	IR (cm^{-1})[a b,c]	NMR[d,e] $^{31}P\{^1H\}$ (ppm)[f]	NMR[d,e] ^1H (ppm)[g, h]	NMR[d,e] $^{13}C\{^1H\}$ (ppm)[h, i]
$[RhOs(CO)_2(\mu\text{-}\eta^3\text{:}\eta^1\text{-}C(CH_2)_3)(dppm)_2][BF_4]$ (**3.1**)	2003 (s), 1929 (s)	40.6 (dm, $^1J_{RhP}$ = 152 Hz), -1.4 (m)	4.39 (m, 2H, dppm), 4.10 (s, 2H), 4.01 (m, 2H, dppm), 1.95 (d, $^3J_{PH}$ = 8 Hz, 2H), 1.79 (t, $^3J_{PH}$ = 12 Hz, 2H)	181.6 (t, $^2J_{PC}$ = 8 Hz, 1C), 172.4 (t, $^2J_{PC}$ = 7 Hz, 1C), 73.5 (t, $^2J_{PC}$ = 7 Hz), 7.27 (s, br)
$[RhOs(CO)_3(\mu\text{-}\eta^3\text{:}\eta^1\text{-}C(CH_2)_3)(dppm)_2]$ $[BF_4]$ (**3.2**)		13.8 (dm, $^1J_{RhP}$ = 137 Hz), -8.1 (m)	4.74 (m, 2H, dppm), 4.31 (m, 2H, dppm), 2.63 (d, $^3J_{PH}$ = 9 Hz, 2H), 2.03 (s, 2H), 1.69 (t, $^3J_{PH}$ = 9 Hz, 2H)	194.7(dt, $^1J_{RhC}$ = 60 Hz, 1C), 185.9 (m, 1C), 177.3 (m, 1C)
$[RhOs(CO)_2(PMe_3)(\mu\text{-}\eta^3\text{:}\eta^1\text{-}C(CH_2)_3)(dppm)_2][BF_4]$ (**3.3**)		14.3 (dm, $^1J_{RhP}$ = 140 Hz), -13.7 (m), -49.8 (d, $^1J_{RhP}$ = 104 Hz)	4.87 (m, 2H, dppm), 4.55 (m, 2H, dppm), 3.21 (s, 2H), 2.07 (t, $^3J_{PH}$ = 11 Hz, 2H), 1.87 (d, $^3J_{PH}$ = 8 Hz, 2H), 1.76 (d, $^2J_{PH}$ = 13 Hz, 9H)	

Table 3.1. Spectroscopic Data For Compounds. (cont'd)

Compound	IR (cm^{-1})[a b,c]	NMR[d,e] $^{31}P\{^1H\}$ (ppm)[f]	^1H (ppm)[g, h]	$^{13}C\{^1H\}$ (ppm)[h, i]
$[RhOs(CO)_2(\mu\text{-}\eta^3\text{:}\eta^1\text{-}CH(CH_3)C(CH_2)_2)(dppm)_2][BF_4]$ (**3.4**)	2001 (s), 1923 (s)	42.8 (m), 36.9 (m), -0.1 (m), -7.2 (m)	4.41 (om, 4H, dppm, $CHCH_3$), 3.9 (m, 1H, dppm), 3.58 (s, 1H, $C(CH_2)CHCH_3$), 2.12 (d, 1H, J_{PH}= 8 Hz CH_2CHCH_3), 2.01 (m, 1H, $^1J_{CH}$= 130 Hz, Os-CH_2), 1.90 (m, 1H, $^1J_{CH}$= 130 Hz, Os-CH_2), -0.22 (dd, 3H, $^4J_{PH}$ = 6 Hz, $CHCH_3$, $^3J_{HH}$ = 6 Hz)	181.2 (m, 1C), 172.7 (m, 1C), 81.9 (dd, 1C, $^1J_{RhC}$= 29 Hz, J_{PC}= 6 Hz, $CHCH_3$), 64.6 (dd, 1C, $^1J_{RhC}$= 32 Hz, J_{PC}= 7 Hz, $C(CH_2)CHCH_3$), 15.6 (s, 1C, CH_3), 9.5 (s, 1C, Os-CH_2)
$[RhOs(CO)_3(\mu\text{-}\eta^3\text{:}\eta^1\text{-}CH(CH_3)C(CH_2)_2)(dppm)_2][BF_4]$ (**3.5**)		11.3 (om), -3.2 (m), -16.2 (m)	5.35 (m, 1H, dppm), 4.82 (m, 1H, dppm), 4.59 (m, 1H, dppm), 4.21 (m, 1H, $CHCH_3$), 4.10 (m, 1H, dppm), 1.35(m, 3H, $CHCH_3$)	184.9 (m), 183.9 (m), 177.1(m), -4.1 (s),

Table 3.1. Spectroscopic Data For Compounds. (cont'd)

Compound	IR (cm^{-1})[a b,c]	NMR[d,e] $^{31}P\{^1H\}$ (ppm)[f]	^1H (ppm)[g, h]	$^{13}C\{^1H\}$ (ppm)[h, i]
$[RhOs(CO)_3(\mu\text{-}\eta^1\text{:}\eta^1\text{-}((CH_3)_2\text{-}C)CH_2CH_2)(dppm)_2][CF_3SO_3]$ (**3.6**)		24.3 (dm, $^1J_{RhP}$ = 121 Hz), -3.2 (m)	4.90 (m, dppm, 2H), 4.07 (m, dppm, 2H), 2.41 (s, br, CH_2, 2H), 1.63 (t, br, Os-CH_2, 2H), 0.78 (t, J = 6 Hz, CH_3, 3H), 0.10 (s, br, CH_3, 3H)	191.4 (dt, $^1J_{RhC}$= 48 Hz, $^2J_{PC}$= 11 Hz), 182.5 (s, br, Os(CO)), 172.8 (t, $^2J_{PC}$ = 8 Hz, Os(CO)), 2.69 (t, $^2J_{PC}$ = 8 Hz)

[a] IR abbreviations: s = strong, m = medium, w = weak, sh = shoulder. [b] CH_2Cl_2 solutions unless otherwise stated, in units of cm^{-1}. [c] Carbonyl stretches unless otherwise noted. [d] NMR abbreviations: s = singlet, d = doublet, t = triplet, m = multiplet, dm = doublet of multiplets, om = overlapping multiplets, br = broad, dt = doublet of triplets. [e] NMR data at 25°C in CD_2Cl_2 unless otherwise stated. [f] ^{31}P chemical shifts referenced to external 85% H_3PO_4. [g] NMR data collected at -80°C in CD_2Cl_2. [h] Chemical shifts for the phenyl hydrogens are not given. [i] ^1H and ^{13}C chemical shifts referenced to TMS. [j] $^{13}C\{^1H\}$ NMR performed with ^{13}C enrichment of both carbonyls and methylene groups.

reaction was observed. Addition of a 5 mL CH_2Cl_2 solution of Me_3NO (3.5 mg, 1.2 equiv) via cannula to the solution of **1.2** and allene, resulted in a colour change from yellow to dark-red. The solution was stirred for 30 minutes, filtered, and a red-orange solid was isolated by the slow addition of 10 mL of ether followed by 20 mL of pentane. The isolated solid was washed with ether and dried under a stream of argon (yield 87%). Anal. Calcd. for $C_{56}H_{50}F_4O_2P_4RhOsB$, C, 51.78; H, 3.89, Found. C, 52.20; H, 3.75 MS-*m/z* 1173 (M^+ - BF_4)

b) **[RhOs(CO)$_3$(μ-η^3:η^1-C(CH$_2$)$_3$)(dppm)$_2$][BF$_4$] (3.2).** Compound **3.1** (30 mg, 0.026 mmol) was dissolved in 10 mL of CH_2Cl_2 and carbon monoxide was passed over the solution for 5 min at a rate of 1 mL/min. The solution slowly turned from red-orange to yellow. The solution was stirred for 30 minutes, filtered, and then a yellow solid was precipitated by the slow addition of 10 mL of ether and 20 mL of pentane. The solid was washed with ether, and dried under a stream of argon (yield 78%). Satisfactory elemental analyses for this compound could not be obtained due to facile CO loss. Characterization is based on spectroscopic studies.

c) **[RhOs(CO)$_2$(PMe$_3$)(μ-η^3:η^1-C(CH$_2$)$_3$)(dppm)$_2$][BF$_4$] (3.3).** Compound **3.1** (30 mg, 0.026 mmol) was dissolved in 0.7 mL of CD_2Cl_2 and cooled to –80° C. An excess of 1.0 M trimethylphosphine in toluene (40 µL, 0.040 mmol, 1.6 equiv.) was added at this temperature. Although no colour change was observed, NMR characterization at –80°C revealed complete conversion to a new product. This product was stable up to –20 °C. However at higher temperatures, facile PMe_3 loss occurred, so it was characterized at low temperature through NMR spectroscopy.

d) Attempted reaction of 3.1 with CH_2N_2. Compound **3.1** (20 mg) was dissolved in 0.7 mL of CD_2Cl_2, and cooled to –80 °C. An excess of diazomethane was passed through the solution at a rate of 10 mL/min for 2 minutes. The reaction was stirred for 20 minutes at low temperature and the excess diazomethane was removed at this temperature. Upon slowly allowing the solution to warm to room temperature, the colour changed from orange to yellow. The NMR spectrum of the solution showed a mixture of unidentifiable products.

e) $[RhOs(CO)_2(\mu\text{-}\eta^3\text{:}\eta^1\text{-}(CH(CH_3)C(CH_2)_2)(dppm)_2][BF_4]$ (3.4). Compound **1.2** (30 mg, 0.024 mmol) was dissolved in 10 mL of CH_2Cl_2 and methyl allene was slowly passed through the solution at a rate of 0.5 mL/min. No reaction was observed. A 2 mL solution of Me_3NO (2.1 mg, 1.2 equiv) was added via cannula to the solution containing both compound **1.2** and methyl allene. The resultant orange solution was stirred for 30 minutes and then filtered. An orange solid was precipitated by the slow addition of 15 mL of pentane, and the isolated solid was washed with 20 mL of ether and dried under a stream of argon (yield 86%). Anal. Calcd. for $C_{57}H_{50}F_4O_2P_4RhOsB$, C, 52.17; H, 3.93, Found, C, 51.88, H, 3.90. MS- *m/z* 1187 (M^+ - BF_4)

f) $[RhOs(CO)_3(\mu\text{-}\eta^3\text{:}\eta^1\text{-}(CH(CH_3)C(CH_2)_2)(dppm)_2][BF_4]$ (3.5). Compound **3.4** (30 mg, 0.025 mmol) was dissolved in 10 mL of CH_2Cl_2 and carbon monoxide was passed through the solution at a rate of 2 mL/min for two minutes. This caused an immediate colour change from orange to yellow. The solution was stirred for 20 minutes and precipitated by the slow addition of 20 mL of ether followed by 10 mL of pentane, filtered, and dried under a stream of argon. This compound was prone to facile CO loss, and thus it was characterized using NMR techniques.

g) Attempted reaction of 3.4 with PMe_3. An NMR tube charged with compound **3.4** (15 mg, 0.013 mmol) was dissolved in 0.7 mL of CD_2Cl_2 and cooled to –80 °C. 25 μL of PMe_3 (0.025 mmol, 1.25 equiv) was added to the solution via syringe. No colour change was observed and the ^{31}P $\{^1H\}$ NMR spectrum of this solution showed only compound **3.4** and unreacted PMe_3.

h) $[RhOs(CO)_3(\mu\text{-}\eta^1\text{:}\eta^1\text{-}C(C(CH_3)_2)CH_2CH_2)(dppm)_2][CF_3SO_3]$ (3.6). Compound **2.1** (20 mg, 0.015 mmol) was dissolved in 0.7 mL of CD_2Cl_2 and cooled to –10°C. To the cooled solution, 1.8 μL (1.2 equiv) of dimethyl allene was added and stirred for 5 minutes. The resultant dark red solution could only be characterized by NMR spectroscopy, as the compound rapidly decomposed at ambient temperature.

Results and Compound Characterization

The addition of the cumulenes, allene, methylallene, and dimethylallene, to the methylene-bridged, tetracarbonyl species $[RhOs(CO)_4(\mu\text{-}CH_2)(dppm)_2][BF_4]$ (**1.2**) has been investigated.[2] While no reaction occurs over a period of one week with either allene or methylallene, dimethylallene reacts slowly over the course of a few days to yield 1,1-dimethyl-1,3-butadiene[1] (established by comparison of its ^1H NMR spectrum to that of an authentic sample) and the well-known complex, $[RhOs(CO)_4(dppm)_2][BF_4]$[2] (**1.1**) as shown in Scheme 3.1 (dppm ligands above and below the plane of the drawing are omitted for clarity). No intermediate in the formation of these products was observed over a range of temperatures from –80°C to ambient.

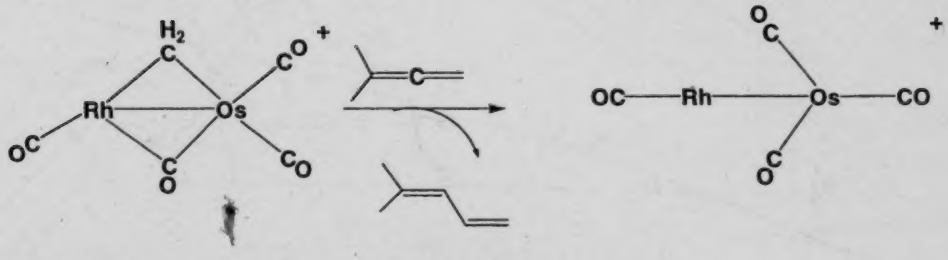

Scheme 3.1. *Reaction of compound 1.2 with dimethylallene.*

Although compound **1.2** is unreactive towards allene and methylallene, the removal of a carbonyl with trimethylamine-N-oxide from **1.2** in the presence of the allenes results in immediate incorporation of allene and methylallene into the resultant tricarbonyl species. Addition of allene to complex **1.2** yields the trimethylenemethane-bridged complex $[RhOs(CO)_2(\mu\text{-}\eta^3\text{:}\eta^1\text{-}C(CH_2)_3)(dppm)_2][BF_4]$ (**3.1**), as shown in Scheme 3.2. This product displays a $^{31}P\{^1H\}$NMR spectrum characteristic of an

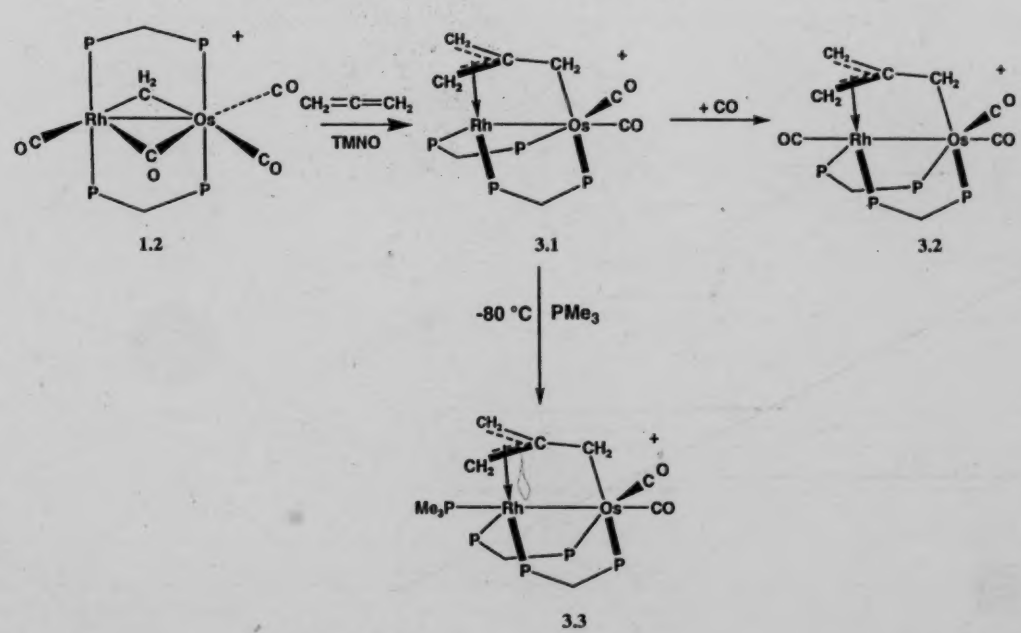

Scheme 3.2. *Reactions of allene with compound 1.2.*

AA'BB' spin system, with a low-field chemical shift at δ 40.6 ($^1J_{RhP}$ =152 Hz) corresponding to the Rh-bound phosphines, and a high field shift at δ –1.4 corresponding to the Os-bound phosphines. In the ^{1}H NMR spectrum, the two signals at δ 4.39 and δ 4.01, corresponding to the dppm methylene groups, indicate two different chemical environments for the two pairs of methylene protons. In the structure shown above these would correspond to one on each dppm methylene group that is oriented towards each other and to the pair (one on each methylene) oriented away from the other diphosphine. Three additional methylene resonances are observed as a triplet at δ 1.79, a doublet at δ 1.95, and a broad singlet at δ 4.10. The triplet corresponds to the methylene protons that is σ-bound to Os and displays 12 Hz coupling to the Os-bound phosphines. The doublet corresponds to a pair of protons on the η^3-allyl portion of the trimethylenemethane group, which display 8 Hz coupling to one of the Rh-bound phosphines, and are *anti* to the Os-bound CH_2 group, while the broad singlet corresponds to the pair of *syn* protons of the allyl moiety. The resonances for the allyl fragment are very similar to those reported for the 2-methylallyl ligand in a series of compounds $Rh(\eta^3\text{-}CH_2C(CH_3)CH_2)(PR_3)_2$[4] in which the geometry at Rh is very similar to that proposed for compound **3.1**.

When the above reaction is repeated using a $^{13}CH_2$-enriched sample of **1.2**, the $^{13}CH_2$ label is found to be uniquely situated in the site that is σ-bound to Os; no scrambling is observed between the three methylene units of the insertion compound. The unique placement of the labelled CH_2 group adjacent to the Os suggests that the insertion of the allene has occurred into the Rh-C bond as observed in all reactions involving alkynes, reported in Chapter 2. An IR spectrum of **3.1** shows the presence of two terminally bound CO stretches at 2003 and 1929 cm^{-1}. Using ^{13}CO, the terminally

bound carbonyls are observed in the $^{13}C\{^1H\}$ NMR spectrum at δ 181.6 and 172.4, and selective decoupling of the phosphines and the absence of Rh-coupling show that they both are bound to osmium. The 2-D HMBC and HMQC experiments were used to aid in the assignment of the trimethylenemethane fragment. Both sets of allylic methylene hydrogens couple to the pair of carbons that resonate at δ 73.5, whereas the protons of the osmium-bound methylene group couples to the carbon that resonates in the ^{13}C NMR spectrum at δ 7.27 in the HMQC experiment. Attempts to assign the quaternary carbon with an HMBC experiment failed, as it did not show the appropriate correlation.

The addition of CO or PMe_3 to **3.1** yields the adducts, $[RhOs(CO)_3(\mu\text{-}\eta^3\text{:}\eta^1\text{-}C(CH_2)_3)(dppm)_2][BF_4]$ (**3.2**) and $[RhOs(CO)_2(PMe_3)(\mu\text{-}\eta^3\text{:}\eta^1\text{-}C(CH_2)_3)(dppm)_2][BF_4]$ (**3.3**), respectively. The ^1H NMR spectra of both compounds display the singlet, doublet, triplet pattern for the trimethylenemethane unit, as observed in **3.1**, with coupling to the phosphines of between 8 and 12 Hz. Although both products are analogous, apparently having the added group on Rh, a notable difference between the two compounds is the initial site of attack of the ligands. Addition of ^{13}CO at –80°C shows that initial attack appears to occur at osmium, with the labelled CO appearing at δ 186.4 in the $^{13}C\{^1H\}$ NMR spectrum, displaying no coupling to Rh. Upon warming to ambient temperature, the label is seen at all three carbonyl sites (δ 194.7, 186.4, and 177.3), with the signal at δ 194.7 showing typical rhodium coupling of 60 Hz. The addition of PMe_3 to **3.1** at –80°C gives rise to a doublet in the $^{31}P\{^1H\}$ at δ -49.4 ppm with a rhodium coupling of 104 Hz, in addition to the signals from the Rh- and Os-bound dppm ligands at δ 14.3 and –13.7 respectively. This clearly demonstrates that the PMe_3 group is bound to Rh even at -80°C so it is assumed that initial attack has occurred here. Warming the sample to

ambient temperature gives rise to no change in the NMR spectrum, as the PMe_3 group remains bound to Rh.

The reaction of **1.2** with methylallene gives a product $[RhOs(CO)_2(\mu\text{-}\eta^3\text{:}\eta^1\text{-}(CH(CH_3)C(CH_2)_2)(dppm)_2][BF_4]$ (**3.4**), that appears to be analogous to **3.1**, in which methylallene insertion into the Rh-CH_2 bond has occurred, as shown in Scheme 3.3. The $^{31}P\{^1H\}$ spectrum of **3.4** appears as a distinct ABCDX pattern, in which all four ^{31}P environments differ. The Rh-bound phosphine signals are two complex multiplets at δ 43.3 and 36.8, while the signals from the Os-bound phosphines are also two multiplets centred at δ 0.93 and -7.63, showing a definite second-order pattern. As shown in Scheme 3.3, the methyl substituent on one end of the allene renders the pair of

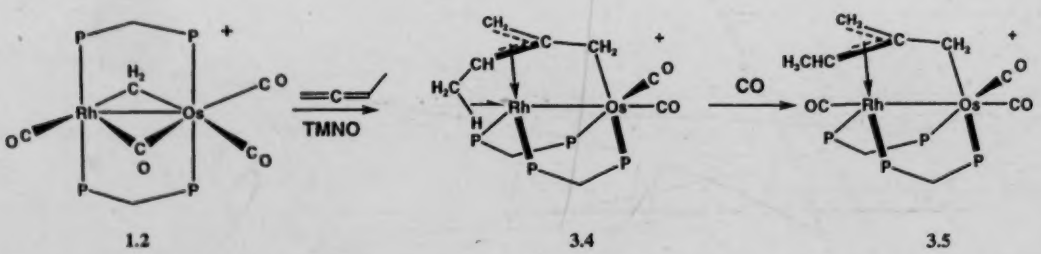

Scheme 3.3. *Reactions of compound 1.2 with methylallene.*

phosphines on each metal inequivalent. Despite this difference in the $^{31}P\{^1H\}$ spectra, the ^1H spectra of compounds **3.1** and **3.4** are quite similar. Here again, the *syn* protons appear as a singlet at δ 3.61 and the *anti* proton as a doublet at δ 2.12 with 8 Hz coupling to the osmium-bound phosphines. Instead of a triplet for the metal-bound methylene, these protons now appear as two multiplets at δ 1.90 and 2.00. When the $^{13}CH_2$-labelled precursor is used, the Os-bound CH_2 protons display coupling to their attached carbon of 130 Hz. The complexity of the proton signals is not surprising since each proton is

coupling to another proton, a phosphine, and in some cases, also to the Rh-centre. The methyl signal appears as a doublet of doublets ($^4J_{PH}$= 6 Hz, $^3J_{HH}$= 6 Hz) at δ -0.22. The unusually high-field shift of this methyl group has led us to speculate that there is an agostic interaction between the it and one of the metals, and that rapid rotation of this methyl group brings each of the C-H bonds into an agostic interaction in turn. Facile methyl rotation in agostic interactions is a common observation in transition metal compounds.[5] For example, Tempel and Brookhart observed in-place rotation of the agostic methyl group in a mononuclear palladium compound [(ArN=(R)CC(R)=NAr)Pd-(CH(CH_2-μ-H)(CH_3))][BAr_4][6]. Here, the agostic methyl signal is broad at both ambient and low temperature (-115°C). Milstein reported an agostic methyl interaction with a Rh centre in a PCN ligand system.[7] In his compound, as has been seen in other literature compounds, the signal for the agostic methyl is a broad singlet, with no coupling to the phosphines observed. The methyl signal in the ^{1}H NMR spectrum of compound **3.4** collapses to a doublet ($^3J_{HH}$= 6 Hz) upon selective phosphorus decoupling of the rhodium-bound phosphines, supporting the proposal that there is indeed an interaction between Rh and the methyl group; surprisingly however, no Rh coupling is observed. The agostic methyl was determined to be *anti* to the methylene group that is σ-bound to Os, assigned by comparison to Fryzuk's series of substituted allyl complexes.[4] The signal for the single proton adjacent to the methyl substituent of the allene moiety was found buried under one of the signals for the dppm methylenes at δ 4.41 through ^{1}H COSY experiments. Again, through the use of **$^{13}CH_2$-1.2**, it is seen that the original methylene group retains its bond to Os with no scrambling between the two different methylene sites; this resonance is now a broad signal found at δ 9.52 in the $^{13}C\{^1H\}$

NMR spectrum. Similar to the allene product, two terminal carbonyls are observed in the $^{13}C\{^1H\}$ NMR spectrum using ^{13}CO at δ 181.2 and 172.0 and the absence of Rh coupling to either establishes that both are bound to Os.

Bridging trimethylenemethane complexes are rare. There have been two reports in the literature of such complexes, one with a diruthenium centre[8] and the other with a mixed-metal tungsten-nickel system.[9] Knox *et al.* reported the diruthenium trimethylenemethane complex, $[Ru_2(CO)_2(\mu\text{-}\eta^1\text{:}\eta^3\text{-}C(CH_2)_3)Cp_2]$ analogous to **3.1**, through the reaction of $[Ru_2(CO)_2(CH_3CN)(\mu\text{-}CH_2)Cp_2]$ with allene. The ^1H NMR spectrum of the diruthenium complex at –60 °C showed six individual signals for each of the protons in the trimethylenemethane moiety. However, upon warming, the signals broadened and coalesced at 70 °C, at which temperature, three equal intensity signals were observed. They also reported the fluxionality of the carbonyls, which allowed the complex to retain its plane of symmetry, which is in direct contrast to our results, which show that the carbonyls are not scrambling. In the NiW system, the ^1H NMR spectrum of the insertion complex, $[NiW(Cp^*)(Cp)(\mu\text{-}CO)_2(\mu\text{-}\eta^1\text{:}\eta^3\text{-}C(CH_2)_3)]$, was reported to display dynamic behaviour. When the temperature of the NMR sample was raised above –20°C, the signals of the three methylene units were found to broaden and collapse. At 95°C, an additional peak appeared at the average chemical shift of the previous three. The authors described rotation in their complex to be occurring about the central, quaternary carbon. This rotation is also commonly observed in mononuclear, trimethylenemethane species,[10] however, both **3.1** and **3.4** spectroscopically show that this rotation does not occur.

The ^{1}H NMR spectra of both **3.1** and **3.4** have a similar pattern; there is a broad singlet, a doublet, and a third signal that is a triplet in **3.1**, but because of the lower symmetry, is a multiplet in **3.4**. This pattern has been seen by Fryzuk in his previously mentioned studies of a mononuclear Rh allyl system,[4] where a low-field singlet appears for the *syn* protons, while the *anti* protons constitute a doublet at higher fields. In these same studies with methyl substituted allyls, Fryzuk comments about the symmetry of the methylallyl derivatives yielding an ABX ^{31}P{^{1}H} NMR pattern, as was described for compound **3.4**. He also remarks that in the ^{1}H NMR spectrum the signals are each multiplets, one for each of the diastereotopic protons in the molecule.

Addition of CO to compound **3.4** results in the formation of $[RhOs(CO)_3(\mu\text{-}\eta^3\text{:}\eta^1\text{-}C(CHCH_3)(CH_2)_2)(dppm)_2][BF_4]$ (**3.5**). At room temperature, the ^{31}P{^{1}H} spectrum displays a broad signal at δ 11.3 from the Rh-bound phosphines, which when cooled shows the signal for the two chemically inequivalent rhodium-bound phosphines as overlapping multiplets at δ 11.3. The osmium-bound phosphines are two multiplets, centred about δ 3.2 and 16.2, and do not show much temperature dependence. The ^{1}H NMR spectrum for **3.5** is quite similar to **3.4**, with most protons appearing as multiplets, except for the singlet and doublet from the methylallene moiety. The methyl signal appears as a doublet of doublets at δ 1.35, still showing phosphine and proton coupling, each of about 6 Hz. It is notable that addition of CO has resulted in a substantial down-field shift of this methyl group from that observed (δ –0.22) in the precursor, suggesting that the CO ligand has replaced the agostic interaction of the methyl group. Attempts to determine the initial site of attack of the CO were unsuccessful; no CO coordination was observed at low temperatures, and when prepared at room temperature and subsequently

cooled, the ^{13}C NMR spectrum shows scrambling of the labelled carbonyl equally through the three carbonyl sites.

As noted earlier, the reaction of compound **1.2** with 1,1-dimethylallene yields 1,1-dimethyl butadiene, with no intermediates being observed in the reaction. In an effort to isolate a possible intermediate en route to the elimination of 1,1-dimethyl butadiene, dimethylallene was reacted with the tricarbonyl compound **2.1**. The product of this reaction, $[RhOs(CO)_3(\mu\text{-}\eta^1\text{:}\eta^1\text{-}((CH_3)_2C(CH_2)_2)(dppm)_2][CF_3SO_3]$ (**3.6**), shown in Scheme 3.4, proved to be difficult to isolate due to its instability upon further work-up. As a result, the compound was characterized *in situ*. In the ^1H NMR spectrum, the dppm methylene groups appear at δ 4.90 and 4.07, indicating the molecule possesses front-back asymmetry. An Os-bound methylene signal appears as a broad triplet at δ 1.63 with 8 Hz

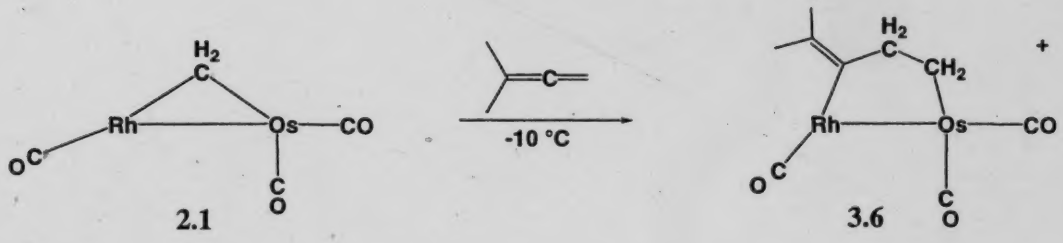

Scheme 3.4. *Reactivity of compound 2.1 with dimethylallene (dppm groups omitted for clarity).*

coupling to the osmium-bound phosphines, while the other methylene signal is a broad singlet at δ 2.43. Phosphorus decoupling results in no change in this latter methylene signal, while selective phosphorus decoupling experiments show sharpening of the signal at δ 1.63 only when the osmium-bound phosphine signal is decoupled, confirming that

insertion has again occurred into the rhodium-carbon bond. The connectivity of the organic fragment was confirmed through a 2-D proton COSY experiment, which shows coupling between the two methylene signals. The lack of phosphorus coupling with the β-methylene group indicates that it is not bound to the metal. The methyl resonances from the allene moiety are at relatively high field. One appears as a triplet at δ 0.78 showing phosphorus coupling to the rhodium-bound phosphines of $^{5}J_{PH}$= 6.4 Hz, and the other is a broad singlet at δ 0.10. From $^{13}C\{^{31}P\}$ experiments carried out with a ^{13}CO-enriched sample of **3.6**, three terminally bound carbonyls are observed; the low field resonance, at δ 191.2 ($^{1}J_{RhC}$= 48 Hz) corresponds to a Rh-bound carbonyl, while the other two, a broad singlet at δ 182.5 and a triplet having 11 Hz coupling to the Os-bound phosphines at δ 172.8, are on the osmium centre. When compound **3.6** is left at ambient temperature for approximately two hours, the ^{31}P $\{^{1}H\}$ NMR spectrum shows approximately 20 % conversion into the tetracarbonyl complex $[RhOs(CO)_4(dppm)_2]^+$ a conversion that is complete after 5 hours. In the ^{1}H NMR spectrum after this time, the resonances from 1,1-dimethylbutadiene can be identified. The additional carbonyl observed in this transformation presumably is scavenged from unidentified decomposition products. Attempts to stabilize complex **3.6** by the addition of PMe_3 or CO resulted in the de-insertion of dimethylallene, and the formation of the previously known complexes $[RhOs(CO)_3(PMe_3)(\mu\text{-}CH_2)(dppm)_2]^+$ [11] or $[RhOs(CO)_4(\mu\text{-}CH_2)\text{-}(dppm)_2]^+$ (**1.2**), respectively.

Discussion

As noted in previous chapters, coupling of methylene groups promoted by the complex $[RhOs(CO)_4(dppm)_2]^+$, was proposed to proceed by stepwise CH_2 insertion into the Rh-CH_2 bond of the different hydrocarbyl-bridged intermediates, (containing sequentially the μ-CH_2, μ-C_2H_4, μ-C_3H_6 groups). We have attempted to model the putative C_3H_6-bridged intermediate in this process by the insertion of unsaturated substrates into the Rh-CH_2 bond of $[RhOs(CO)_x(\mu\text{-}CH_2)(dppm)_2]^+$ (x= 3, 4). In this chapter, we have described the reactions of these methylene-bridged precursors with allene, methylallene, and 1,1-dimethylallene. Assuming that allene attack at Rh and subsequent insertion into the Rh-CH_2 bond occurs, two initial insertion products are expected, as shown in structures **E** and **F** in Chapter 1. In this proposal, it is also assumed that allene coordination will occur at the unsubstituted double bond and not at the substituted end. It appears that in this chemistry described, both modes of insertion occur, although only one is stable.

The reactions of allene and methylallene with compound **1.2** yield the same type of product, whereas dimethylallene yields a different product. Allene yields the dicarbonyl, trimethylenemethane-bridged species $[RhOs(CO)_2(\mu\text{-}\eta^1\text{:}\eta^3\text{-}C(CH_2)_3)(dppm)_2][BF_4]$ (**3.1**) in which the trimethylenemethane group is σ-bound to Os *via* one CH_2 group and bound as an η^3-allyl group through the remaining $C(CH_2)_2$ moiety. This trimethylenemethane-binding mode has been seen before in both mono and bimetallic systems. One of the earliest examples of a monometallic system is from 1972, where Emerson and Ehrlich studied a trimethylenemethaneiron tricarbonyl complex.[12] There have been many examples of mononuclear trimethylenemethane species reported. Sita

and co-workers studied models for the Ziegler-Natta process using cationic and zwitterionic allyl-Zr complexes that were derived from trimethylenemethane cyclopentadienylzirconium complexes.[13] Wojcicki *et al.* have also reported Pt and Pd trimethylenemethane complexes that are susceptible to nucleophilic attack.[14] In addition to monometallic studies, there have also been studies on the reactivity of bimetallic complexes. Trimethylenemethane fragments at a bimetallic core have previously been generated as described in this chapter by the insertion of allene into an $M(\mu\text{-}CH_2)M$ moiety. So for example, the reaction of $[Ru_2(CO)_2(MeCN)(\mu\text{-}CH_2)Cp_2]$ with allene gives the product $[Ru_2(CO)_2(\mu\text{-}\eta^1\text{:}\eta^3\text{-}CH_2C(CH_2)_2)Cp_2]$, having the trimethylenemetane moiety in a bridging role. We assume that in our study, the allene coordination at Rh occurs with subsequent insertion into the Rh-CH_2 bond to yield intermediate **E** (See Scheme 1.8), having the unsaturated group on the central carbon of the C_3-bridged unit. However, this group can be viewed as an η^1-allyl group with respect to both metals, with rotation about the bond linking the Os-bound CH_2 group and the β-carbon transforming the η^1-allyl group into an η^3-allyl, with concomitant loss of a carbonyl (Scheme 3.5).

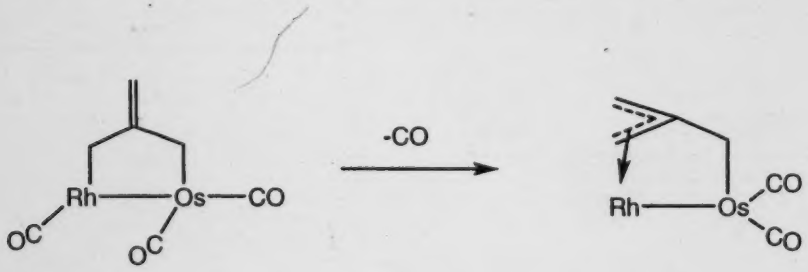

3.1

Scheme 3.5. *Conversion from an η^1-allyl to an η^3-allyl group.*

In order to transform the η^1-allyl to the η^3 mode, one of the metal-carbon σ-bonds needs to be broken, and one of the carbonyls must be lost. Both of these steps occur at the

rhodium centre with retention of the Os-CH_2 bond in both complexes. This observation is attributed to the stronger osmium-carbon bond versus the rhodium-carbon bond. The strong Os-C σ-bond can also be credited for the lack of fluxionality seen among the methylene units of our compounds. The proposed transformation of an η^1- to an η^3-allyl with accompanying carbonyl loss suggested that addition of ligands such as CO and PMe_3 might effect the reverse η^3- to η^1-coordination mode of the allyl moiety. Although, coordination of both of these groups occurs, it happens with retention of the η^3-allyl binding mode. In compound **3.1** the Rh centre has a $16e^-$ configuration, so incorporation of a $2e^-$ donor can occur without the need to lose the favoured η^3 coordination of the allyl fragment. Surprisingly, the site of attack of the CO and PMe_3 in compound **3.1** differs. The site of phosphine attack at Rh is expected, based on the coordinative unsaturation at this metal. However, carbonyl attack at the saturated Os centre (as seen by labelling studies at -80°C) was unexpected. Presumably, movement of a bound carbonyl from Os to Rh is followed by CO attack at Os. We assume that the phosphine fails to attack at osmium for steric reasons and is more favoured at Rh.

Attempts to initiate further C-C bond formation by incorporating additional methylene groups into **3.1** (by the reaction of diazomethane) failed, as no reaction was observed under a variety of conditions.

It is interesting to note that the reaction of allene and the methylene-bridged tetracarbonyl complex (**1.2**) will not proceed without the addition of TMNO, nor will it proceed from a sample of isolated methylene-bridged tricarbonyl (**2.1**). The reaction of **2.1** and allene yields only a mixture of unidentified products, even when carried out at low temperatures. Instead, formation of **3.1** only occurs through the *in situ* generation of

the tricarbonyl species from its tetracarbonyl precursor in the presence of allene. This observation suggests that some complexation involving allene with the tetracarbonyl species must occur, allowing the desired reaction to take place upon carbonyl loss.

Compound **1.2** reacts with methylallene in a manner quite like that of allene, yielding the methyl-substituted trimethylenemethane-bridged product **3.4**. In this product, the methyl substituent participates in an agostic interaction with the Rh, giving this metal an 18e$^-$ configuration. A notable difference between the two complexes **3.1** and **3.4** is their reactivity towards nucleophiles. While CO adds to **3.4** readily at room temperature displacing the agostic interaction, it does not add at lower temperatures, presumably being unable to displace the agostic methyl interaction at the lower temperature. Using ^{13}CO, carbonyl scrambling is observed at temperatures near ambient. However, we could not determine the site of CO attack in this case since reaction was not observed at temperatures below which scrambling occurs. Surprisingly, PMe_3 does not add to the complex, possibly because the extra steric demands of the methyl substituent on the allyl moiety does not permit close approach of the phosphine ligand to the rhodium centre. Using labelled **2.1-$^{13}CH_2$** in the reaction of **3.1** and **3.4** produced $^{13}C\{^1H\}$ NMR spectra that exhibited no scrambling among the CH_2 groups. In a related diruthenium system, this was also seen.[8]

In contrast to both allene and methylallene, which did not react with the tetracarbonyl complex **1.2**, dimethylallene (DMA) reacts slowly with this species. Previous studies of the reaction of (DMA) with $[RhOs(CO)_4(\mu\text{-}CH_2)(dppm)_2][CF_3SO_3]$ (**1.2**) established that over the course of a few days conversion to *trans*-1,1-dimethyl-butadiene and the known tetracarbonyl complex $[RhOs(CO)_4(dppm)_2][CF_3SO_3]$ (**1.1**)

occurred.[1] No intermediate was seen by NMR spectroscopy over the course of this reaction. The DMA was speculated to react at Rh, as with the other allenes in compound **2.1**, inserting into the rhodium-carbon bond to yield a product similar to **E**, described in Chapter 1 and shown as **P** in Scheme 3.6. β-hydrogen elimination followed by reductive elimination of the hydride and alkenyl fragment are proposed to yield the dimethylbutadiene product. This initial insertion product **P** is differs from that

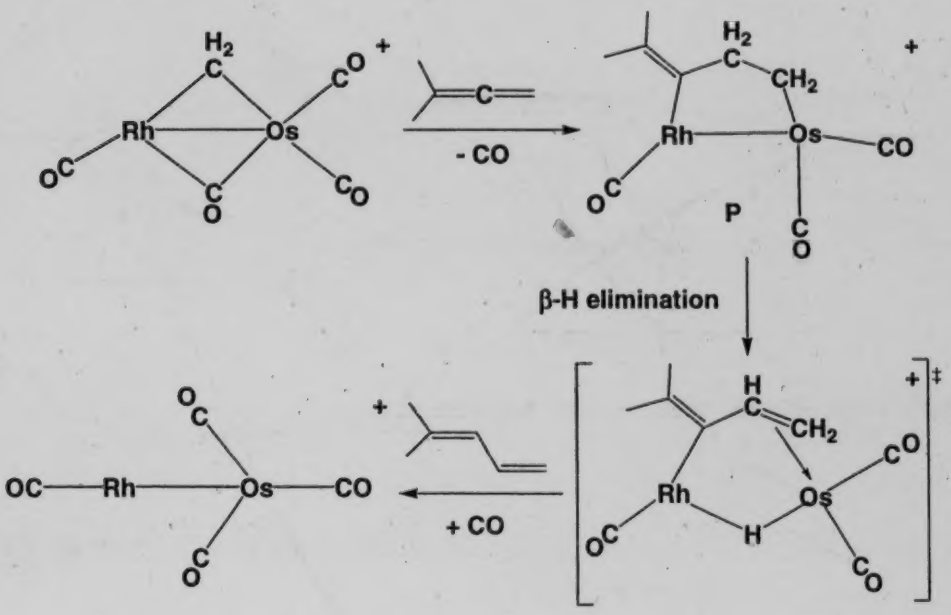

Scheme 3.6. *Proposed mechanism for the elimination of trans-1,1-dimethylbutadiene. (dppm groups omitted for clarity).*

proposed in the reactions with allene and methylallene. This difference is attributed to the steric demands of the dimethylallene ligand, which presumably favours the alternate initial π-adduct, leading to the other insertion product. Although no intermediates were observed in the transformation shown in Scheme 3.6, the proposed was isolated

intermediate by the reaction of the tricarbonyl species **2.1** with DMA. This species $[RhOs(CO)_3(\mu\text{-}\eta^1\text{:}\eta^1\text{-}((CH_3)_2C(CH_2)_2)]^+$ (**3.6**), has been characterized at low temperatures but it is unstable at room temperature, decomposing in a matter of hours to give 1,1-dimethylbutadiene.

Our studies on mixed-metal complexes necessitate investigating different metal combinations in order to establish the roles of the various metals and of the *combinations* of metals. It is therefore useful to compare what has has been described above with that observed for the Rh/Ru combination of metals. The reaction of allene[15] with $[RhRu(CO)_3(\mu\text{-}CH_2)(dppm)_2]^+$ proceeds in essentially an identical manner to that described above in our studies with the RhOs combination of metals, demonstrating that in this case, substitution of Os for Ru has little obvious affect on the reactivity. In this example, the reactivity is dominated by substrate coordination and insertion at Rh to yield the stable products. However, a surprising difference is observed with 1,1-dimethylallene in reactions with the Rh/Os and Rh/Ru combinations of metals. Whereas the Rh/Os system generated 1,1-dimethylbutadiene as described above, the Rh/Ru system yielded the carbonyl insertion product **S** shown in Scheme 3.7. We propose that, as described earlier for Rh/Os, the initial product in the Rh/Ru complex is the insertion product **Q**. This is exactly analogous to the labile product **3.6** observed with Rh/Os. Whereas with Rh/Os, the next step is proposed to be β-hydrogen elimination, this is apparently not favoured in the Rh/Ru system. Substituting the third-row Os for the second-row Ru not only makes the system less prone to the C-H bond-cleavage step, but this change in metals also favours alkyl migration to give the acyl intermediate **R**.[16] Migration of the Ru-bound acyl to Rh is presumably favoured by the resulting 5-membered metallacycle

that is formed, which is less strained than the 6-membered dimetallacycle in **R**, and is further favoured by donation of a pair of electrons on the acyl oxygen to alleviate the electronic unsaturation at Ru.

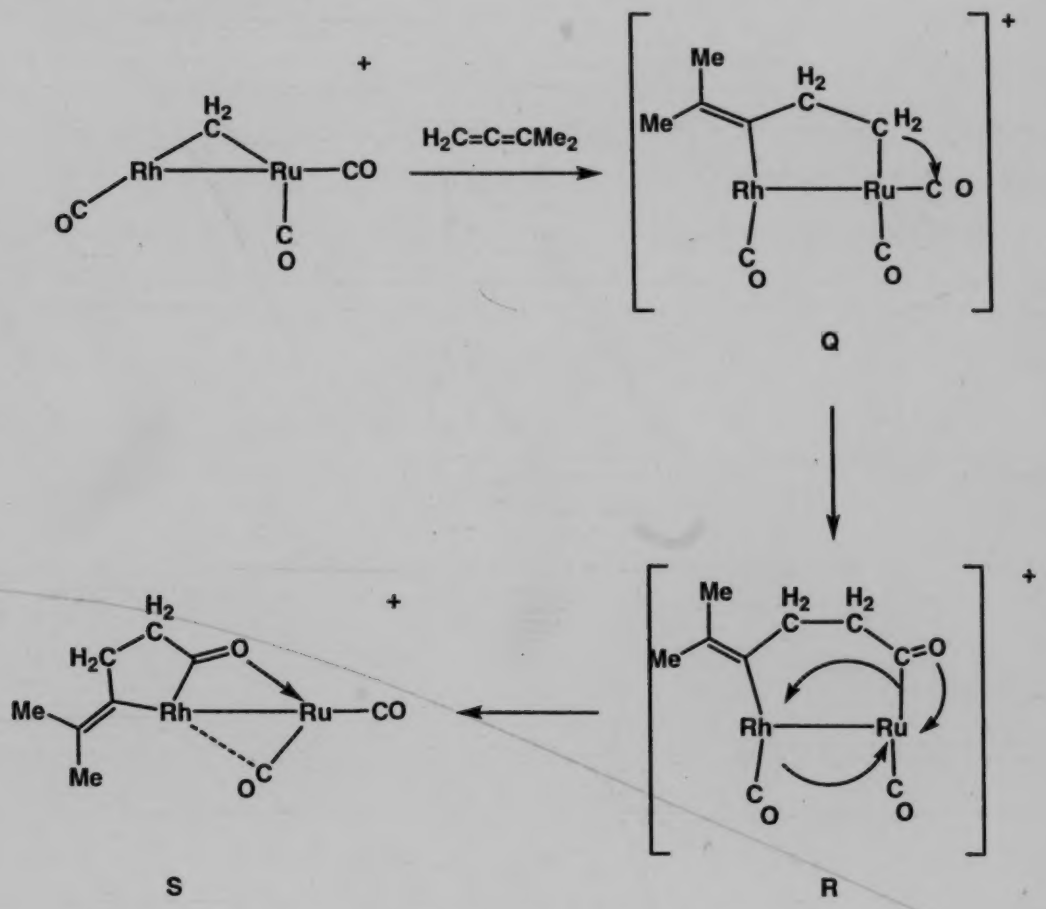

Scheme 3.7. *Proposed mechanism for the reaction of dimethylallene with a Rh/Ru complex (dppm groups omitted for clarity).*

Conclusions

A primary goal of the studies on the reactivities of the methylene-bridged complexes **1.2** and **2.1** with allenes was to generate model C_3-bridged species like those described in Chapter 2, and to study subsequent C-C bond formation in these products. This goal has been realized only in a limited sense in the reaction of the tricarbonyl species **2.1** with dimethylallene, in which a C_3-bridged product **3.6** was observed and characterized, although subsequent incorporation of methylene groups was not possible. In the cases of the other cumulene molecules (allene and methylallene), the goal was not realized. The proposed insertion product **F**, described in Chapter 1, was not observed. However, these products are suggested as the initial products of insertion that subsequently rearranged to the more stable species in which η^3-binding of part of the trimethylenemethane moiety was observed. This binding is not common, although it has been observed previously in bimetallic systems.

In all cases, the initial product is one in which the cumulene has inserted into the Rh-C bond. This is consistent with the findings reported in Chapter 2 and with our other reports. As stated in Chapter 1 (see Scheme 1.8), allene insertion may follow one of two paths, and it was our assertion that the absence of β-hydrogens in the substrate could lead to additional stability of the product. In this chapter, both products **E** and **F** were reported as either seen or proposed as an intermediary step, and it was shown that when insertion occurs such that β-hydrogen elimination is possible (compound **3.6**), the final product is not as stable.

At the outset of this study, it was proposed that different combinations of metals as catalysts could influence the distribution of products in **FT** reactions. A comparison of

the reactivities of the Rh/Os and Rh/Ru combinations of metals with 1,1-dimethylallene sheds some light on this proposal, at least for homogeneous systems. As described, the Rh/Os combination of metals results in coupling of the cumulene with a bridging methylene group, ultimately yielding 1,1-dimethylbutadiene whereas the Rh/Ru metal combination yields a metal-bound acyl product, which under appropriate conditions could presumably be liberated from the metals as an oxygenate product. It is anticipated that other interesting contrasts in the chemistries of these two pairs of metal combinations will be observed.

References and Notes

1. Trepanier, S.J., *Ph. D. Thesis*, University of Alberta, Edmonton, Alberta, **2002**.
2. Trepanier, S.J.; Sterenberg, B. T.; McDonald, R.; Cowie, M. *J. Am. Chem. Soc.* **1999**, *121*, 2613.
3. Trepanier, S.J.; Dennett, N.L.; Sterenberg, B.T.; McDonald, R; Cowie, M. *Manuscript to be Submitted.*
4. Fryzuk, M.D. *Inorg. Chem.* **1982**, *21*, 2134.
5. (a) Brookhart, M.; Green, M.L.H.; Wong, L. *Prog. Inorg. Chem.* **1988**, *36*, 1. (b) Brookhart, M.; Green, M.L.H. *J. Organomet. Chem.* **1983**, *250*, 395.
6. Tempel, D.J.; Brookhart, M. *Organometallics* **1998**, *17*, 2290.
7. Gandelman M.; Shimon L.J.W.; Milstein, D. *Chem.-A Eur. J.* **2003**, *9*, 4295.
8. Fildes, M.J.; Knox, S.A.R.; Orpen, A.G.; Turner, M.L.; Yates, M.I. *J. Chem. Soc., Chem. Commun.* **1989**, 1680.
9. Chetcuti M.J.; Fanwick, P.E.; Grant, B.E. *Organometallics* **1991**, *10*, 3003.

10. Albright, T.A.; Hofmann, P.; Hoffmann, R. *J. Am. Chem. Soc.* **1977**, *99*, 7546.

11. Wigginton, J.R; Trepanier, S.J.; Ferguson, M.J.; McDonald, R.; Cowie, M. *Manuscript to be Submitted.*

12. Ehrlich K.; Emerson G.F. *J. Am. Chem. Soc.* **1972**, *94*, 2464.

13. Kissounko, D.A.; Fettinger, J.C.; Sita, L.R. *J. Organomet. Chem.* **2003**, *683*, 29.

14. Dunsizer, R.T.; Marsico, V.M.; Plantevin, V.; Wojcicki, A. *Inorg. Chim. Acta*, **2003**, *342*, 279.

15. Rowsell, B.D.; Cowie, M. *Unpublished results.*

16. Allen, F.H.; Kennard, O.; Watson, D.G.; Brammer, L.; Orpen, A.G.; Taylor, R. *J. Chem. Soc. Perkin Trans. II*, **1987**, S1.

Chapter 4

Conclusions and Future Work

The goal of this thesis was to synthesize C_3-bridged complexes containing the Rh/Os combination of metals as models for $(CH_2)_n$-containing (n= 1-4) intermediates that have been prepared by the coupling of methylene groups promoted by the cationic species, $[RhOs(CO)_4(dppm)_2]^+$ (**1.1**).[1] This methylene-coupling reaction also paralleled a proposal by Mark Dry[2] for the chain-propagation steps in the **FT** reaction. Although there has been significant work done in modeling the **FT** reaction by using binuclear homogeneous complexes,[1,3] primary interest of the Cowie group lies in the use of mixed-metal complexes as models for bimetallic **FT** catalysts and in the use of easy-to-study models to determine the roles of the different metals in carbon-carbon bond formation and in other processes of relevance to **FT** chemistry. Although homogeneous complexes have commonly been used to model **FT** chemistry, few studies have been carried out by other groups on mixed-metal systems. The strategy for generating C_3-bridged models was through coupling of methylene groups as C_1 fragments and alkynes or allenes as C_2 fragments. Two simple strategies for generating C_3-bridged complexes would involve reaction of the appropriate methylene-bridged complex with C_2 fragments or reaction of C_2-bridged fragments with diazomethane. Subsequent increases in the length of the hydrocarbyl fragment could, in principle, be generated by further addition of either C_1 or C_2 fragments. It was our hope to first obtain a better understanding of coupling of hydrocarbyl fragments at two adjacent metals and a better understanding of the roles of the different metals in these processes. Furthermore, since the hydrocarbyl fragments

were those proposed to have significance in the **FT** reaction, it was hoped that such studies could ultimately shed light on mechanistic details of this important processes.

Although not all of the strategies attempted were successful with respect to the above goals, we did have an encouraging amount of success, and also generated interesting chemistry even for the results that did not directly address the defined goals. The reactions involving alkynes were the most successful in addressing our goals of synthesizing model C_3-bridged complexes and of moving sequentially from C_2- to C_3-bridged and from C_3- to C_4-bridged species.

Using the highly reactive tricarbonyl species $[RhOs(CO)_3(\mu\text{-}CH_2)(dppm)_2]^+$ (**2.1**) and the alkynes DMAD and HFB, the targeted C_3-bridged products $[RhOs(CO)_3(\mu\text{-}\eta^1\text{:}\eta^1\text{-}(R)C{=}C(R)CH_2)(dppm)_2]^+$ (R= CO_2CH_3 (**2.2**) or CF_3 (**2.3**)) were isolated and fully characterized. The resulting C_3 fragments have the "$RC{=}C(R)CH_2$" moiety bound in an η^1:η^1 bridging mode in which Rh binds to the terminal vinylic carbon and Os binds to the methylene group, indicating that insertion into the Rh-CH_2 bond has occurred. Not only does the η^1:η^1 binding mode effectively model that of the propanediyl fragment proposed in the Rh/Os-promoted methylene-coupling reaction[1] and the same fragment proposed by Dry in his **FT** scheme, the insertion at Rh also confirms previous proposals within the Cowie group[1,4] that substrate activation occurs at Rh with subsequent insertion occurring into the Rh-C bond.

The success at converting one of these C_3 fragments, "$(MeO_2C)C{=}C(CO_2Me)\text{-}CH_2$" into a C_4 fragment by addition of an additional CH_2 group to give $[RhOs(CO)_3(\mu\text{-}\eta^1\text{:}\eta^1\text{-}CH_2(MeO_2C)C{=}C(CO_2Me)CH)(\mu\text{-}H)(dppm)_2]^+$, completes our modeling of the transformation of C_1 to C_3 to C_4 fragments in the above-mentioned methylene-coupling

reaction. Although this C_4 fragment has shortcomings as a model for the butanediyl fragment, due to C-H activation that was not observed with only methylene groups, it raises some interesting questions about how the unsaturation in the central C-C bond of the C_4 fragment leads to their difference in chemistry. This question remains to be answered.

Having an unsymmetrical C_3-fragment with a vinylic group bound to Rh and a saturated methylene group bound to Os begs the question of what reactivity differences might occur if this were reversed. We achieved this reverse binding model by the insertion of a diazomethane-derived methylene group into the Rh-C bond of a bridging alkyne. Warming this species under an excess of diazomethane did not give an observable C_4 product, but yielded a product $[RhOs(CO)_3(\mu\text{-}\eta^1\text{:}\eta^1\text{-}(MeO_2C)C{=}C\text{-}(CO_2Me))(\mu\text{-}CH_2)(dppm)_2]^+$ in which loss of the original methylene group occurred to regenerate a bridging alkyne group. This transformation is also of interest in that it probably helps to answer questions about the differences in reactivity at the different metals. Although unproven at this stage, we propose methylene insertion into the Rh-CH_2 bond to give a $RhCH_2CH_2C(R){=}C(R)Os$ moiety which then extrudes ethylene. Further studies will be needed to determine the mechanism of CH_2 loss. If this is the case, the lability of the Rh-CH_2 bond compared to the stronger Os-CH_2 bond may help rationalize the facile ethylene loss. Additional evidence for the importance of the stronger Os-CH_2 bond is found in a comparison of the chemistry of $[RhOs(CO)_3(\mu\text{-}\eta^1\text{:}\eta^1\text{-}(R)C{=}C(R)CH_2)(dppm)_2]^+$ with its Rh/Ru analogue. Whereas carbonyl loss from the latter results in a substantial rearrangement of the hydrocarbyl framework, possibly initiated by the weaker Ru-CH_2 bond, the Rh/Os analogue retains the coordination mode

of the hydrocarbyl fragment. Presumably, the strong Os-CH_2 bond does not allow the bond cleavage necessary for rearrangement.

Late in this study it was observed that reaction of the alkyne- and methylene-bridged complex $[RhOs(CO)_3(\mu\text{-}\eta^1\text{:}\eta^1\text{-}(MeO_2C)C{=}C(CO_2Me))(\mu\text{-}CH_2)(dppm)_2]^+$ with diazomethane apparently incorporated *three* additional methylene groups, as determined by NMR and MS studies. It is important to investigate this further to determine the nature of the hydrocarbyl product obtained. No other system so far studied in this (or any other group) has shown the versatility in methylene coupling that the Rh/Os system displays. Clearly, more work is necessary to determine why this metal combination is so effective.

In Chapter 3, cumulenes were tested as other potential substrates to generate the models putative C_3H_6 intermediate, noted earlier. These compounds were chosen based on their minimal steric demand and their two readily available π-systems. It was shown that allene, methylallene, and 1,1-dimethylallene were able to insert into the Rh-CH_2 bond of **2.1**, much as shown for the alkynes in Chapter 2. Although the initial reactivity appeared to proceed as predicted, only the dimethylallene reaction generated the targeted η^1:η^1-binding mode for the C_3 product. This species, $[RhOs(CO)_3(\mu\text{-}\eta^1\text{:}\eta^1\text{-}((CH_3)_2C{=}\underline{C}CH_2\underline{C}H_2)(dppm)_2]^+$ (**3.6**) is unstable, decomposing by β-hydrogen elimination followed by reductive elimination to give 1,1,-dimethyl-1,3-butadiene. Again this is an interesting contrast to the analogous Rh/Ru system that yielded the acyl-containing $[RhRu(CO)_3(C(O)CH_2CH_2C(=C(CH_3)_2)(dppm)_2][CF_3SO_3]$ product. We propose that both reactions give rise to the analogous η^1:η^1-C_3-bridged species, but that whereas Os promotes the β-hydrogen elimination reactions, the second-row Ru promotes

migration of the Ru-bound alkyl end of the C_3 fragment to a carbonyl leading to the oxygen-containing fragment.. This gives support to our suggestion that the use of different metal combinations can give rise to different product types- a concept that is of interest from the point of view of rationally modifying product distribution in **FT** chemistry.

Insertion of allene and methylallene occur with a different regiochemistry than with 1,1-dimethylallene, presumably a function of the larger steric bulk of the latter dictating its orientation upon coordination to Rh, which ultimately dictates the geometry of the insertion product. Although we did not observe the targeted C_3-bridged species in this case, which presumably has the unsaturated moiety at the central carbon to give a "$CH_2C(=CHR)CH_2$" moiety (R= H, Me), the subsequent products are consistent with this proposal. The above C_3 moiety is an η^1-allyl group so rearrangement to an η^3-allyl group should not be a surprise, given the stability of the latter over the former; as often demonstrated.[5] We have not succeeded in effecting further methylene incorporation into these species, but the novelty of these products were nonetheless of interest. Attempts to make allene-bridged complexes have failed when attempted with the tetracarbonyl complex **1.1**. This reaction should be re-investigated via removal of a carbonyl from compound **1.1** in the presence of the cumulene ligand, and subsequent reaction of allene-bridged precursors with diazomethane should also be investigated.

The contents of this thesis, taken together with other work done in the group on the same combination of metals and with Rh/Ru, certainly point to the pivotal theme in the chemistry- that the unsaturation at Rh allows facile ligand coordination at this metal, and the lability of the Rh-C versus the Os-C bond allows facile insertion of many added

substrates into adjacent Rh-C bonds. Although the strength of the resulting Os-C bonds seems to also play an important function in the chemistry, and can account for some of the differences observed between Rh/Os and Rh/Ru analogues, other work in the group has demonstrated that more subtle effects can come into play related to the strengths of the respective metal-metal bonds and the nature of bridging ligands.[1,4,6]

It has become clear that a thorough understanding of the roles of adjacent metals in the activation of substrates by heterobinuclear complexes requires not only a careful, methodical study of one metal combination (e.g. Rh/Os) but careful comparisons to related systems containing other combinations of metals (eg. Rh/Ru, Ir/Ru, Ir/Os). A great deal remains to be done before we have the level of understanding required to rationalize even this limited series of mixed-metal complexes. The next question will be whether such studies will have relevance to heterogeneous systems containing the same combination of metals. Clearly, there are many important differences between metal surfaces and the complexes studied through this thesis; the ligands, by virtue of their steric bulk and of their electronic properties must exert important effects not mimicked on a surface.

It is maintained that much can be learned about the nature of organic reactions occurring on a metal surface by parallel studies on complexes such as the ones presented. In particular the presence of adjacent metals in these complexes allows the modelling of the reactivity of substrates that bridge adjacent metals on a surface.

References and Notes

1. Trepanier, S.J.; Sterenberg, B.T.; McDonald, R.; Cowie, M. *J. Am. Chem. Soc.* **1999**, *121*, 2613

2. Dry, M. E. *Appl. Catal. A* **1996**, *138*, 319

3. (a) Torkelson, J.R.; McDonald R.; Cowie M. *J. Am. Chem. Soc.* **1998** *120*, 4047. (b) Trepanier, S.J.; McDonald, R.; Cowie, M. *Organometallics* **2003** *22*, 2638. (c) Maitlis, P.M; Long, H.C.; Quyoum, R; Turner, M.L.; Wang, Z.Q.; *Chem. Commun.* **1996**, *1*, 1. (d) Turner, M.L.; Long, H.C.; Shenton, A.; Byers, P.K.; Maitlis, P.M. *Chem.-Eur. J.* **1995**, *1*, 549.

4. Rowsell, B.D.; Trepanier, S.J.; Lam, R.; McDonald, R.; Cowie, M. *Organometallics* **2002**, 21, 3228.

5. (a) Solin, N.; Szabo, K.J. *Organometallics* **2001**, *20*, 5464. (b) Crabtree, R. H. *The Organometallic Chemistry of the Transition Metals*, Wiley: New York, **1994**. (c) Hegedus, L. S. *Transition Metals in the Synthesis of Complex Organic Molecules*; University Science Books: Mill Valley, CA, **1999** p 245.

6. (a) Ristic-Petrovic, D.; Anderson, D.J.; Torkelson, J.R.; McDonald, R.; Cowie, M. *Organometallics* **2003**, *22*, 4647. (b) Rowsell, B.D.; McDonald, R.; Ferguson, M.J.; Cowie, M. *Organometallics,* **2003**, *22*, 2944. (c) Ristic-Petrovic, D.; Wang, M.; McDonald, R.; Cowie, M. *Organometallics,* **2002**, *21*, 5172. (d) Dell'Anna, M.M.; Trepanier, S.J.; McDonald, R.; Cowie, M. *Organometallics,* **2001**, *20*, 88.

Appendix

Solvents and Drying Agents

Solvent	Drying Agent
CH_2Cl_2	P_2O_5
THF	Na/benzophenone
Et_2O	Na/benzophenone
Pentane	Na/benzophenone

All solvents were distilled from their respective drying agents under an atmosphere of dinitrogen in order to exclude oxygen.